COIL DESIGN FOR LOW FIELD NMR EXPERIMENTS AND NMR MEASUREMENTS ON THE HUMAN ARM

By

THOMAS RICHARD LIGON

Bachelor of Science

Oklahoma State University

Stillwater, Oklahoma

1964

Submitted to the faculty of the Graduate School of
the Oklahoma State University
in partial fulfillment of the requirements
for the degree of
MASTER OF SCIENCE
May, 1967

COIL DESIGN FOR LOW FIELD NMR EXPERIMENTS AND

NMR MEASUREMENTS ON THE HUMAN ARM

Thesis Approved:

V. L. Pollak

E. E. Kohnke

N. N. Durham
Dean of the Graduate School

ACKNOWLEDGMENTS

I wish to thank Dr. V.L. Pollak for his help and guidance, and for the opportunity to undertake the investigation of muscle water; this work was found to be most interesting. I am indebted to the following people who with unflinching patience served as subjects for the arm measurements: Mr. Rodney Schultz, Mr. David West, Mr. Bill McCollum, Jr., and especially to Mrs. Joseph F. Long.

TABLE OF CONTENTS

Chapter		Page
	INTRODUCTION	1
I.	PROXIMITY EFFECT AND THE USE OF STRANDED WIRE	4
	Proximity Effect	4
	Stranded Wire	7
II.	DESIGN OF THE NEW COILS	9
	Notes on the Construction of the Coil	16
	Measurements	16
	B/I Calculation and Measurements	20
III.	CONCENTRIC BUCKING COILS	23
	Design of the Concentric Bucking Coil	24
	Evaluation of Concentric Bucking	27
IV.	INTRODUCTION TO PROTON RELAXATION IN MUSCLE	31
V.	THE EXPERIMENT	35
	Anatomy of the Arm	35
	The Measurements	39
VI.	THE RESULTS OF FOREARM MEASUREMENTS	43
VII.	UPPER ARM MEASUREMENTS	52
	Measurements of Proton Relaxation in Blood	58
	Summary	64
	General Remarks	65
	A SELECTED BIBLIOGRAPHY	67
	APPENDIX	68

LIST OF FIGURES

Figure		Page
1.	Twisting of a Wire Strand Pair to Reduce Losses	7
2.	Specifications for One of the Old Coils	9
3.	Diagram Showing Symbols Used in Comparison of a Solid Wire and a Stranded Wire Coil	13
4.	Circuit Used for Q Measurements	17
5.	Coil Q vs. Frequency	19
6.	Diagram Showing Symbols Used in Field to Current Ratio Expression	21
7.	B/I for Coil Along Axis	22
8.	B/I for Coil Transverse to Axis	22
9.	Diagram of Two Concentric Coils	23
10.	Diagram Defining Symbols Used in Area-Turns Expression	25
11.	Noise Pickup for Coils as a Function of Orientation; Rotation in Plane of Coil Axis	30
12.	Noise Pickup for Coils as a Function of Orientation; Rotation in Plane Perpendicular to Coil Axis	30
13.	Diagrams Illustrating Experiments 1 and 2	40
14.	T_1 vs. Larmor Frequency; Forearm	44
15.	Typical T_1 Data from the Forearm	45
16.	Determination of Forearm Water Volume	50
17.	Analysis of T_2 Data for Determination of Arm Water Volume	54
18.	T_1 vs. Larmor Frequency--Two Component Analysis	59
19.	T_1 vs. Larmor Frequency--Intermediate Exchange Analysis	60

20. T_1 vs. Larmor Frequency for Best Straight Line Analysis 61

21. Typical T_1 Data With Graphical Analysis 62

22. T_1 vs. Larmor Frequency--Cow Blood 63

INTRODUCTION

Two unrelated subjects comprise this thesis. That presented first deals with the theory design and construction of induction coils used in earth's field free precession type of nuclear magnetic resonance experiments. The second topic is the investigation, by making NMR measurements on the human arm, of the nuclear magnetic relaxation times for the protons of water in muscle.

The induction coil which is of interest here is a large air-cored coil which in the earth's field NMR technique serves a dual purpose: first to magnetically polarize a sample under study; second to pick up the precession signal from the component of magnetic moment perpendicular to the earth's field after sudden removal of the polarizing field. The coils described herein were to be similar to coils previously used but with a substantial improvement in Q, and consequently in the signal-to-noise ratio. This improvement was brought about by the use of twisted and stranded wire in place of the solid bell wire which was used in the old coils. The stranded wire allowed a reduction in proximity effect losses in the coil to the extent that the ac resistance of the coil at 2.3 KHz (the Larmor precession frequency of protons in the earth's field), became of the order of the dc resistance of the coils.

Actually two coils are required for such experiments. One performs the above-mentioned functions while a second, so designed that ambient electromagnetic noise picked up by both coils is the same, is wired in series and aligned antiparallel with the first so that this noise is cancelled or "bucked" out. Two sets of coils were constructed. The first consists of two identical coils; the second set uses a concentric bucking arrangement-- a center coil identical to one of the coils in the first set and two outer coils in a Helmholtz arrangement for the bucking coil.

The objectives sought in the second section of this thesis were to investigate the possibility of using a human or perhaps an animal limb for NMR measurements on muscle and to extend information on proton relaxation times in muscle gained by other workers to fields lower than had previously been used.

Bratton, Hopkins and Weinberg (1965), using high field NMR equipment and with a sample of frog muscle wired for artificial stimulation, have reported finding a field dependence for T_1 (the longitudinal relaxation time) for the protons of water in the muscle, and have found that the transverse relaxation time, T_2, is dependent upon the state of the muscle. T_2 was found to increase with tetanic isometric contraction and with exhaustion of the muscle over that value of T_2 found for the relaxed muscle. At the same time no field dependence was found for T_2, and T_1 appeared to be independent of the state of the muscle. These measurements were carried out at two field strengths corresponding to Larmor frequencies of 24.0 MHz and 4.3 MHz. In the paper by Bratton, Hopkins and Weinberg, three possible models were suggested that might acount for their results. Their data was applied to the most attractive of these with somewhat inconclusive results.

The earth's field apparatus seemed ideal in some respects for extending this work. The two great advantages are that measurements of relaxation times can be made over a wide range of field strength, and sample preparation is convenient.

CHAPTER I

PROXIMITY EFFECT AND THE USE OF STRANDED WIRE

Losses due to the skin effect and proximity effect are both attributable to eddy currents. In the skin effect, eddy currents are caused by the fluctuating magnetic field present when a conductor is carrying an ac current. The magnetic field lines for an isolated wire of circular cross section are circles concentric about the axis of the wire and existing in the wire as well as externally to it. Eddy currents will circulate in such a manner that the main current is augmented near the surface of the wire and is reduced toward the center. The result is that as the frequency is increased the current tends to be restricted to the surface area of the wire. The exclusion of current in the center of the wire requires also the absence of any magnetic field in the interior so that the depth to which there is appreciable current is also that depth to which the magnetic field effectively penetrates.[1] For an examination of the skin effect from a field point of view, see Welsby (1960), pp. 46-52.

Proximity Effect

The term "proximity effect" refers to losses in a conductor which

[1]The attenuation of the current in the wire is of the form $I=I_0e^{-ax}$ where I_0 is the current density at the surface of the wire and x is the distance radially into the conductor. The depth of penetration is usually defined as that depth at which the current density is attenuated to 1/e, or one neper, of its value at the surface.

is under the influence of fields originating external to it. When two wires are lying side by side and carrying an ac current, the magnetic field affecting one is the vector sum of its own field plus that due to the other. This enhanced field in the interior of the wires gives rise to proportionally larger eddy currents representing greater losses. The current distribution is no longer radially symmetric about the center of the conductor but will become more concentrated toward one side as the frequency is increased. Formulas exist for computing the proximity effect resistance for various cases such as two wires in parallel, two wires in a return circuit, wires carrying current differing in phase, three wires, etc. (Dwight, 1945)

In the 1920's the radio industry was in its adolescence and there was a great need for good design formulas for radio frequency coils. Outstanding pioneers in this work were S. Butterworth and R.G. Medhurst. Early efforts resulted in successful formulas for such relatively simple systems as groups of conductors and idealized coils, but real coils, i.e. multilayer solenoids, were too complicated.[2] The development of useful formulas required some empiricism; coils were actually constructed and measurements carefully made on them.

In a multilayer coil of the type which is of interest here, the magnetic field which most turns experience is perpendicular to the axis of the wire, and the frequency is low enough that skin effects are negligible. Eddy currents induced circulate in such a manner to concentrate the cur-

---

[2]When skin effect is not negligible the field external to the wire is modified in the vicinity of the wire, leading to a rather complicated situation for the purposes of mathematical analysis. Bessel functions must be used and as the system becomes more complex the computation quickly becomes impossibly difficult.

rent on one side of the wire, thus effectively increasing its resistance. Since over the winding cross section of a coil the flux density B varies, so too does the ac resistance of any given turn. Those turns near the center and on the core of a multilayer solenoid offer the greatest resistance while the outermost turns account for the least losses.

In Welsby's The Theory and Design of Induction Coils, the following expression for the ac resistance (R_e) of a coil is derived:

$$R_e = \beta \lambda d^2 f^2 L \qquad \text{eq. 1.}$$

λ is the packing factor (ratio of total wire cross sectional area to coil cross sectional area) of the coil, d is the diameter of the wire in centimeters, f is the frequency and L is the inductance of the coil in henrys. β is a constant for a given coil and is dependent upon the quantity $\left(\frac{H_{mean}\ell}{NI}\right)$ where H_{mean} is the mean field intensity averaged over the winding area, ℓ is the total length of wire, N is the number of turns and I is the rms current in the wire. It is in the evaluation of this quantity that empiricism plays an important part. Butterworth published expressions from which the quantity $\left(\frac{H_{mean}\ell}{NI}\right)$ can be calculated for multilayer solenoid coils. In Welsby's book this is given as a plot so that for a coil of given dimensions the value of β can be found. L needs to be known, and expressions for inductance of a coil will be discussed later. Upon examination of eq. 1 an obvious way to decrease R_e would be to use smaller diameter wire, that is wire with thick insulation. This would also decrease λ so that if small wire of diameter d is used instead of wire of larger diameter D, R_e would be reduced by a factor $\frac{d^4}{D^4}$. However the dc resistance of the coil will be increased by a factor $\frac{D^2}{d^2}$.

Stranded Wire

A common approach by which eddy current losses are minimized is to modify the conductor to increase the resistance for the eddy currents. This may be accomplished by subdividing the conductor in the direction of the eddy flow (e.g. the lamination of transformer cores). If a wire in a coil is simply stranded then the losses are the sum of the losses in each individual strand plus losses resulting from eddy current circulation from one strand to another via the end connections. This latter contribution may be eliminated by the axial twisting of the stranded wire. How this is so may be seen by referring to the diagram in Figure 1. In part (a) there are two strands connected at their end points and these wires are in a uniform alternating magnetic field in a direction perpendicular to the page. This is the same situation as far as eddy currents are concerned as a coil wound with wire of two strands and untwisted if the field of the coil were uniform over the volume of the coil. Each of the individual strands will have in their bulk circulating eddy currents and in addition there will be a flow of eddy current as indicated by the arrows during one half-cycle when the field is increasing and into the page. This latter current is directly proportional to the flux enclosed by the two strands, the induced e.m.f. in the circuit being equal to the time rate of change of the flux in the area enclosed

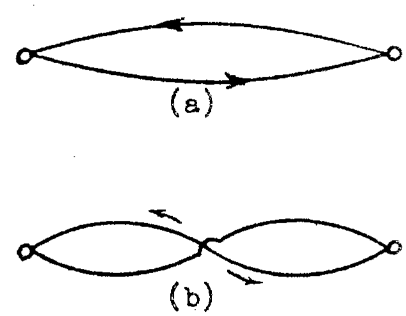

Figure 1. Twisting of a wire strand pair for eddy current reduction.

by the two strands, and by Lenz's law it is in such a direction as to oppose the changing flux that gives rise to it. If one end of the pair of strands is twisted a half turn relative to the other as is depicted at (b), then the induced currents, which would circulate in the same sense in each loop, tend to cancel each other out. If the flux intercepted by each loop is the same, that is if their areas are the same and the field is uniform, then the cancellation is complete. Loops formed by any two strands in a multistranded twisted wire present equal areas to the flux so that this cancellation can be thought of as taking place in pairs of strands. The requirement that two successive loops of the twisted wire be in a uniform field can be met if there is at least half a twist in each turn of the coil. For a more complete discussion of twisting, the reader is referred to Welsby (1960), pp. 54-55 and chapter IV.

With this portion of the eddy current taken care of by axial twisting, there remains only those losses in each individual strand. Then the ratio of the ac resistance of a coil to its inductance, wound with stranded and twisted wire, is the same as in a coil wound with a solid wire of the same diameter of a strand in the first, with length the same as the total length of the strands and with the same dimensions. Comparing the losses, or the ac resistance as given by eq. 1, of the two identical coils, one wound of solid wire diameter D, and the other with stranded and twisted wire with strand diameter d, for the second coil R_e is less by a factor $\frac{d^2}{D^2}$ over the first if the difference in the packing factor, λ, is neglected.

CHAPTER II

DESIGN OF THE NEW COILS

Previously two sets of coils had been constructed; the second pair was to differ from the first in that it consisted of seven sections to reduce the self-capacitance of the coils. These coils were not put into use because of their low inductance. The dimensions and electrical specifications of one of these coils is given in Figure 2. L and R_{dc} were

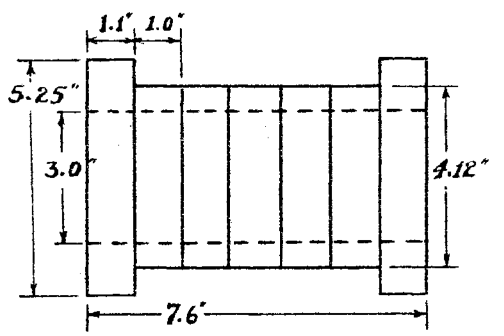

Dimensions given for section width are approximate. 0.1 inch thick spacers separate the sections. There are 285 turns in an end section and nominally 120 in a small section.

$L = 43.2$ mh $R_{dc} = 3.4$ ohms
$Q = 27$ (at 2.3 KHz)
$f_s = 62$ KHz (self-resonant frequency)

Figure 2. Specifications for one of the old coils.

measured on a General Radio portable impedance bridge. Q was measured by a method to be discussed later.

Requirements for the new coils other than a high Q were:

1. The same core diameter as the old coils so that sample containers previously used could continue to be used.
2. The proportions for the new and old coils should be about

the same.

3. The dc resistance should be about the same as for the old coils for the reason of compatibility with the existing circuitry used for the control of the polarizing current.

Like the second coils, these coils were to consist of seven sections each.

If two coils are otherwise identical except that the first is wound of stranded wire with n number of strands and the second is wound with solid wire, the ratio of the ac resistance of the first to that of the second is:

$$\frac{R_{e_1}}{R_{e_2}} = \frac{L_1 \beta_1 \lambda_1 {d_1}^2 f^2}{L_2 \beta_2 \lambda_2 {d_2}^2 f^2}$$

where the subscript 1 refers to the coil with stranded wire and the subscript 2 refers to the coil with solid wire. β is dependent only upon the proportions of a coil, so $\beta_1 = \beta_2$. $L_1 = L_2$ if the stranded wire bundle is about the diameter of the solid wire so that the number of turns of the two coils is equal. Then

$$\frac{R_{e_1}}{R_{e_2}} = \frac{\lambda_1 {d_1}^2}{\lambda_2 {d_2}^2} \qquad \text{eq. 1.}$$

Now the packing factor of the coil wound with solid wire is:

$$\lambda_2 = \frac{N \pi {d_2}^2}{4A}$$

where N is the number of turns and A is the cross sectional area of the coil, that is the coil's length times the winding depth. For the coil wound with stranded wire the packing factor is:

$$\lambda_1 = \frac{N n \pi {d_1}^2}{4A}$$

Then eq. 1 becomes:

$$\frac{R_{e1}}{R_{e2}} = \frac{nd_1^4}{d_2^4} \qquad \text{eq. 2.}$$

If it is further required that the cross sectional area of the stranded wire is equal to the cross sectional area of the solid wire, or $nd_1^2 = d_2^2$, then eq. 2 becomes:

$$\frac{R_{e1}}{R_{e2}} = \frac{1}{n} \ .$$

This latter requirement will in itself prohibit the conditions $L_1 = L_2$ and the number of turns in the two coils being equal from being possible simultaneously; however the error resulting from this assumption will surely be small enough for present purpose, which is to choose a suitable strand number and to have some idea of how much reduction in ac resistance can be expected. The ac resistance of the old coils was 19.1 ohms; then

$$R_{e1} = \frac{19.1}{n} \ .$$

Strand number should be a close-packed number so that the stranded wire will have a minimum resistance for the space it occupies; also this will minimize the error in assuming that the two coils could have the same packing factor. Suitable strand numbers are then 7, 19, 37, etc. Nineteen was chosen to be the number of strands; this would give an expected ac resistance of about 1 ohm or only about 30% of the dc resistance. The strand number 37 was rejected because the small increase in coil Q that it would afford would possibly not be worth the disadvantages there might be in using a wire of so many fine strands-- more likely strand breakage, shorting of strands, etc. Also there was some concern about the increased wire surface area in using many strands; if in the fabrication of the wire there is some contamination with ferromagnetic particles from the extruding die, then it would be desirable to keep the total surface area of the wire in the coil from being too great.

The strand size used was AWG #27, for nineteen times its cross sectional area comes closest to the cross sectional area of AWG #14. In the discussion above the insulation thickness was ignored. The insulation was to be a film type, perhaps formvar; for a heavy film the insulation accounts for about 5% of the diameter of AWG #14, and about 12% of the diameter of AWG #27.

To get a better idea of the improvement in Q that could be expected using 19/27 stranded wire instead of 14 gauge solid wire, calculations for Q were made for two coils, one wound with the stranded wire and the other with solid. The additional layers in the end pieces of the coils were considered to be uniformly distributed over the entire length of the coils; the length and core diameter of each were to be 7.1 and 3 inches respectively, and the dc resistance of each was to be 3.4 ohms. The coils were not considered to be composed of sections. The calculation would also serve as a check for the formulas used, since the calculated values for the solid wire coil could be compared to the measured values for such important quantities as Q, the inductance and the ac resistance.

Dividing 3.4 ohms by the linear resistance of each type of wire gave the length of wire required for each coil.

For both coils the diagram below defines the symbols used for various dimensions:

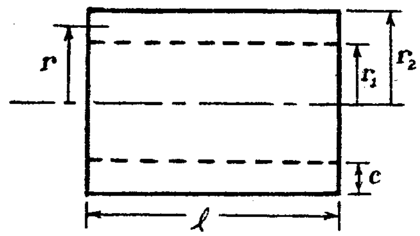

Figure 3. Coil used for calculations.

For the coil with 14 gauge wire:

W = total length of wire = 1345 feet
d = diameter of wire with insulation = 0.066 inches.

From the previous coils about 4% of the winding thickness was unaccounted for by the wire thickness, so the diameter of wire used in calculataion was 0.0678 inches.

Other relationships used were:

$W = 2\pi N r$ where $r = \frac{1}{2}(r_1 + r_2)$
$N = \frac{\ell c}{d^2}$ = the number of turns.

From this:

$$r_2 = \left(\frac{Wd^2}{\pi \ell} + r_1^2\right)^{\frac{1}{2}} .$$

The packing factor, λ, for this coil would be:

$$\lambda = \frac{N\pi d^2}{4\ell c} .$$

From these equations the following values for the coil were calculated:

r_2 = 2.38 inches
c = 0.88 inches
N = 1320 turns
λ = 0.681
r = 1.94 inches

For the inductance the expressions found in Welsby (1960), pp. 42 and 44 were used; they are:

$$L = \frac{4\pi^2 r^2 N^2}{\ell} K_n \, 10^{-9} \text{ henrys } (r \text{ and } \ell \text{ in cm.})$$

where K_n is a correction factor for multilayer solenoids and

$$K_n = \frac{1}{1 + 0.9(\frac{r}{\ell}) + 0.32(\frac{c}{r}) + 0.84(\frac{c}{\ell})} .$$

The inductance of this coil was then calculated to be 60.7 mh. Since the extra windings on the end pieces were considered to be distributed over the length of the coil. thus making a more compact coil, the inductance found by calculation would be expected to be somewhat greater than for one of the real coils.

The equation used for the ac resistance of the coil was

$$R_e = L\beta\lambda d^2 f^2$$

and was discussed in the previous section. Q for this coil was

$$Q = \frac{\omega L}{R_e + R_{dc}}$$

and was calculated for a frequency of 2.3 KHz to be 28.2. This is very near the measured value for Q for the second coil, which was 27.6, so it was hoped then on the basis of this that the calculated Q for the coil with stranded wire would be a realistic value.

Calculations for the coil with stranded wire are the same as the above except in this case the packing factor is:

$$\lambda = \frac{Nn\pi d^2}{4\ell c}$$

where N is the number of turns and n is the number of strands. Also the diameter of the stranded wire is considered to be five strand diameters. Results of the calculations were:

$$
\begin{aligned}
L &= 1255 \text{ feet} \\
r_1 &= 2.55 \text{ inches} \\
c &= 1.05 \text{ inches} \\
r &= 2.03 \text{ inches} \\
\lambda &= 0.476 \\
N &= 1180 \text{ turns}
\end{aligned}
$$

From these values, further calculations gave:

$$
\begin{aligned}
L &= 52.5 \text{ mh} \\
R_e &= 0.93 \text{ ohms at } 2.3 \text{ KHz} \\
Q &= 175 \text{ at } 2.3 \text{ KHz}
\end{aligned}
$$

The decrease in inductance of this coil compared to the previous one reflects the fewer number of turns possible if the dc resistance is to be held to 3.4 ohms. Actually, at least as many turns will be needed for the stranded wire coil to be constructed in order to assure a sufficiently high inductance.

On the basis of the above calculations it was expected that the Q of the coil that was to be constructed would be better by a factor of around 6 over the coils previously used.

The coil winding form used for the previous coils was to be used, and so each section would have a width of 1.1 inches. Five times the strand diameter with insulation was taken as the diameter of the stranded wire, and this would then allow layers of thirteen turns for each section. The previous coils had nominally 120 turns in each section, and thirteen into 120 would give nine layers required. Ten layers was chosen as a better number of layers to insure a sufficiently high inductance. The number of layers for the end sections was to be twice that in the smaller sections plus one layer, or 273 turns. Then with the calculation of the expected winding thickness for the end sections and the smaller sections, the total length of stranded wire required was calculated. This was 1310 feet which should have a dc resistance of 3.5 ohms.

Notes on the Construction of the Coils

When winding of the sections was actually begun, it was found that thirteen turns fit well in the first layer on the coil form, but due to the way successive layers lay on each other, the second and every other even numbered layer took twelve turns. If ten layers were wound, there would then be 125 turns in each small section rather than 130. It was then decided that eleven layers might be better; the dc resistance would be increased somewhat, but it was felt that the increase in inductance afforded would make it worth while. Each small section would then have 138 turns and the end sections 288.

The wire used was 19/27 with Polythermaleze 200 (polyester) film insulation, and it was purchased from the New England Electric Wire Co. of Lisbon, New Hampshire. A coating of epoxy was put on each layer of the sections as they were wound, and the outer and final layer of each section was well sealed with epoxy. The control of the number of turns in each section got better as experience in winding was acquired; a few sections out of the fourteen wound (seven for each coil) had one or two turns more or less than the 138 or 288 desired, but most had the right number.

The expected inductance for a single section was calculated with the equations given above and excellent agreement was found with the measured values. The inductance for the small sections was with some small variation, 1.9 mh, and for the end sections 9.1 mh.

Measurements

The inductance and the dc resistance of the coils was measured on a General Radio portable impedance bridge, and for inductance an external signal generator set at 2.3 KHz was used with the bridge. Singly the inductance of the two coils was:

$$L_1 = 52.5 \text{ millihenrys}$$
$$L_2 = 52.6 \text{ millihenrys}$$
$$R_{dc} \text{ (for both)} = 4.2 \text{ ohms.}$$

With the coils in series and bucking (that is anti-parallel) the inductance was 106.5 millihenrys.

The following circuit was used for determining the Q of the coils:

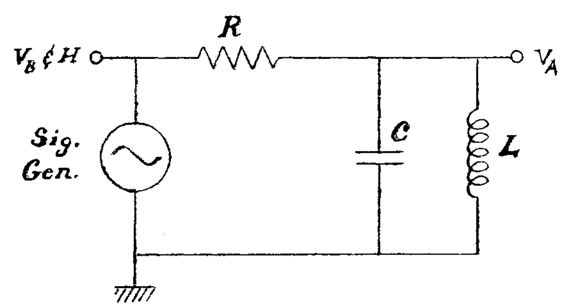

Figure 4. Circuit for Q measurement.

The subscripts A and B refer to the two channels of the dual-trace oscilloscope preamplifier used. C was a polystyrene capacitor of very low loss, R was an appropriate value and carefully measured resistor, and the signal source was a Hewlett-Packard model 200 signal generator. The generator voltage was applied to both vertical channel B and to the horizontal amplifier so that phase differences introduced by the scope amplifiers themselves as frequency was varied could be checked. Fourteen values of capacitance were used for C, corresponding to resonances from 840 Hz to 22.5 KHz for one coil alone. For each value of capacitance the signal generator was adjusted for resonance, and this occurred when the displayed ellipse due to the voltage at point A and that at point B either closed, indicating the tuned circuit was purely resistive, or at the higher frequencies when the ellipse could be matched to that due to the same input (point B) into both horizontal amplifier and vertical amplifier so that what phase difference there was between the two signals was introduced by the scope amplifiers only.

If V is the voltage at point A (the voltage across the tuned circuit), and H is the voltage at point B (the generator voltage), then H-V is the voltage dropped across the resistor R. The impedance of the tuned circuit at resonance is then:

$$z = \frac{V}{H-V} R .$$

To account for the effects of the input resistance of the scope amplifiers losses in the tuning capacitor and the self-capacitance of the coil, the following expression is used to compute the Q of the coil:

$$Q = \frac{z X_c R_{in}}{X_L \left(X_c R_{in} - z X_c - z R_{in} \delta\right)}$$

$X_c = \frac{1}{\omega C}$
R_{in} = input resistance of scope
$X_L = \omega L$
δ = dissipation factor for tuning capacitor

This expression is derived in the appendix. If these influences in the measurement of z are negligible then the Q is simply

$$Q = \frac{z}{X_L} .$$

Only for one coil were measurements made for a plot of Q vs. frequency (see fig. 3). For the other coil and for the coils antiparallel,

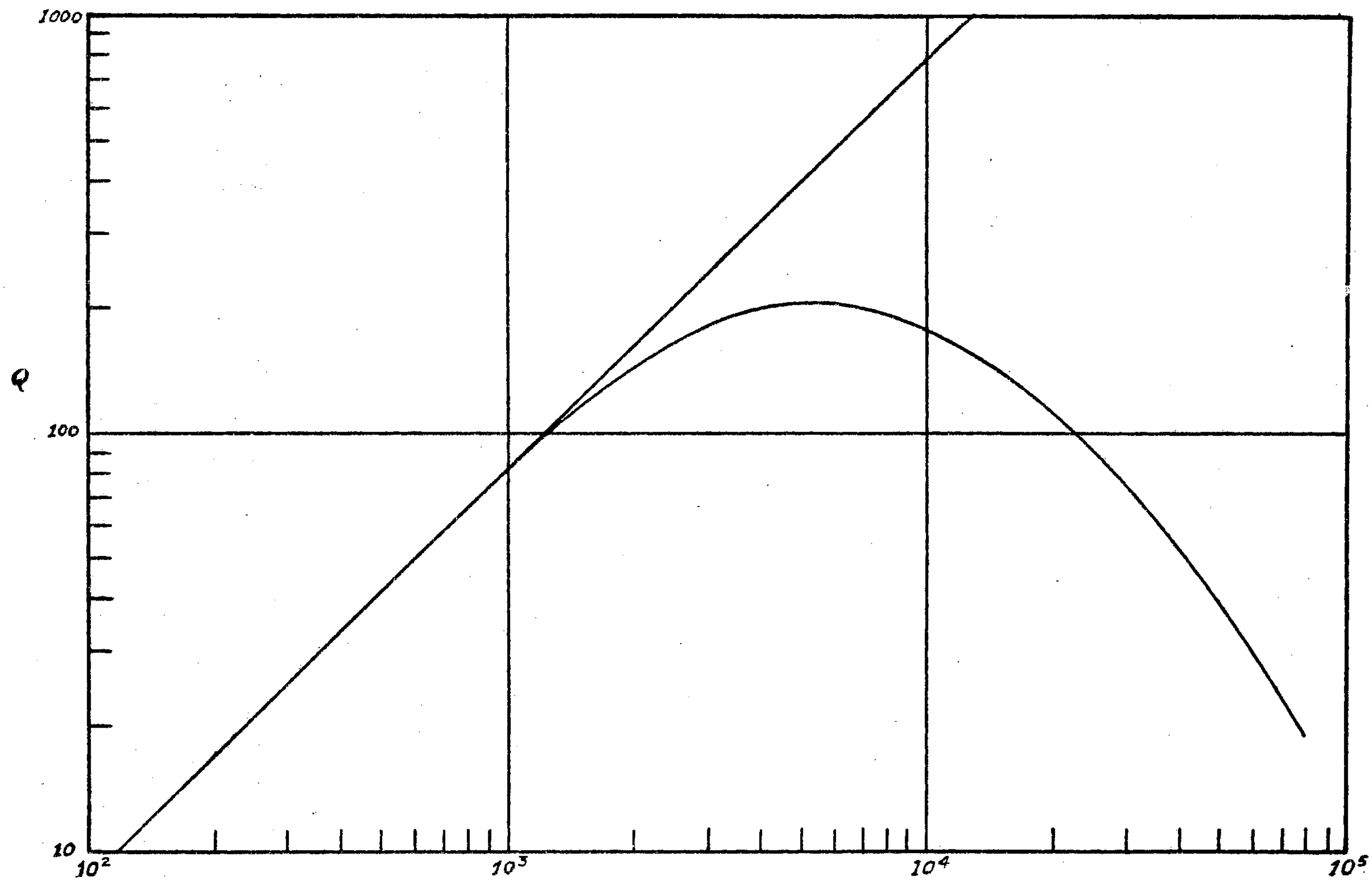

Figure 5. Q versus frequency for one of the new coils. The straight line represents the Q if there were no ac resistance.

Q was found for several frequencies on either side of 2.3 KHz.

The Q for both coils separately at 2.3 KHz was 154; for the coils in series and antiparallel the Q was 148 at 2.3 KHz. The self-resonant frequency of the one coil alone was about 80 KHz corresponding to a self-capacitance for the coil of about 75 pf, and for the two coils together the corresponding values were 46 KHz and 113 pf.

From design considerations of the coils it was determined that an increase of a factor of six for the Q could be expected for the new coils compared to the old, and this factor turned out to be by measurement 5.6.

B/I Calculation and Measurement

When polarizing a sample for NMR measurements it is necessary to know accurately the flux density of the polarizing field. If B/I or the flux density per unit current is known for the coil, then a simple measurement of the polarizing current is all that is needed.

An expression for B/I along the axis for a simple multilayer coil was derived. The expression is exact in the sense that it is for a coil of finite thickness and length. The expression is:

$$B/I = \frac{N\mu_o}{2LC}\left(b+\frac{L}{2}\right)\ln\left[\frac{r_2+\sqrt{r_2^2+(b+\frac{L}{2})^2}}{r_1+\sqrt{r_1^2+(b+\frac{L}{2})^2}}\right]+\left(b-\frac{L}{2}\right)\ln\left[\frac{r_1+\sqrt{r_1^2+(b-\frac{L}{2})^2}}{r_2+\sqrt{r_2^2+(b-\frac{L}{2})^2}}\right]$$

Symbols used are defined by the diagram on the next page.

B/I was calculated for each section for a point on the axis and at the center of the coil and the results summed. The value found was 58.7 gauss/amp for B/I at the center of the coil.

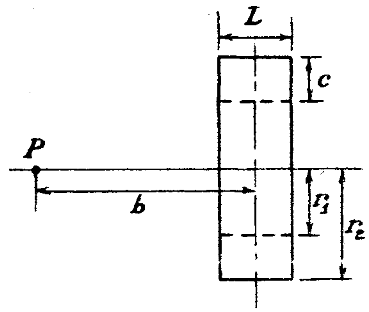

Figure 6. Diagram for B/I expression.

A Bell Model 300 gaussmeter was used to measure the field in the coil while the current was measured with a Simpson precision VOM. A sufficient number of measurements was made to plot B/I along the axis of the coil and transverse to the axis at the venter of the coil and at about the inner edge of each end section (see Figures 7 and 8). Heating of the gaussmeter probe by the coil was a problem, particularly at the points near the inside surface of the coil. Many measurements were made at each point at different times and using different ranges on the gaussmeter; an electric fan was positioned to circulate air through the core and the probe was removed from the coil between each measurement for points off the axis. Discrepancies between B/I on the exis in Figures 7 and 8 are due to the fact that B was measured along the axis on two different gaussmeter ranges and the values averaged, while measurements transverse to the axis were taken with only one range. From the plot the value for B/I at the center and on the axis is 59.3 gauss/amp, in disagreement with the calculated value by about 1%.

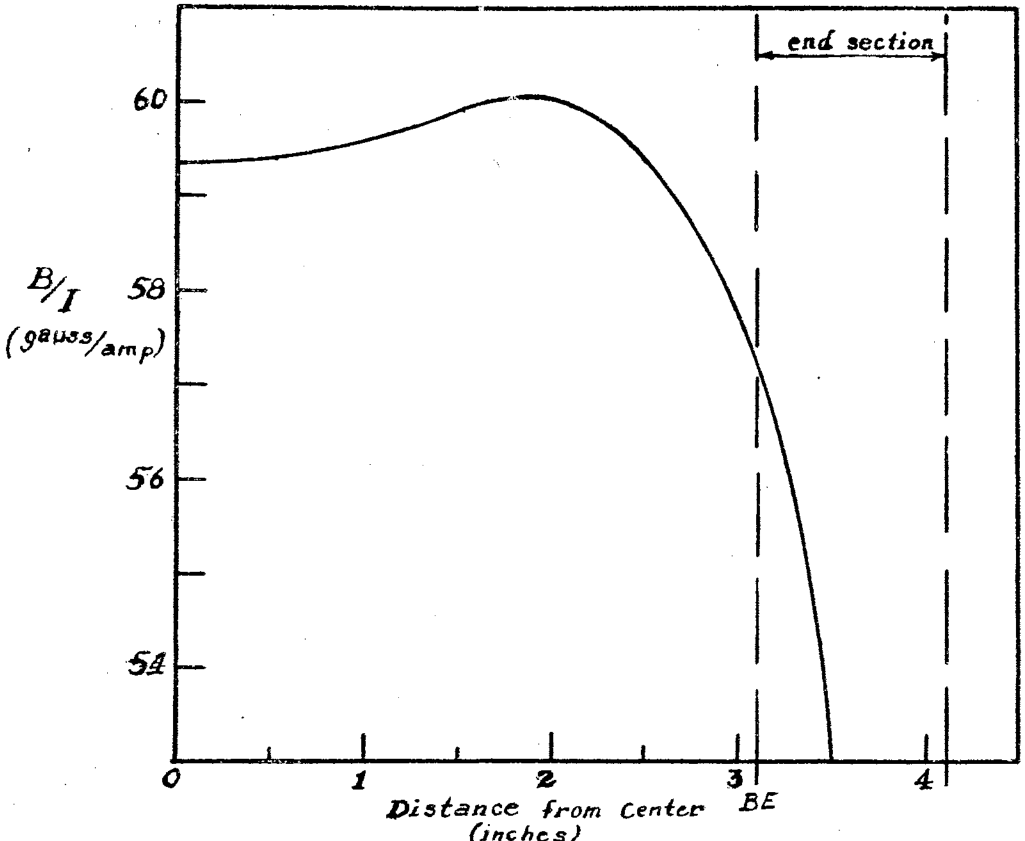

Figure 7. B/I parallel to the axis along the axis of the coil measuring from the center.

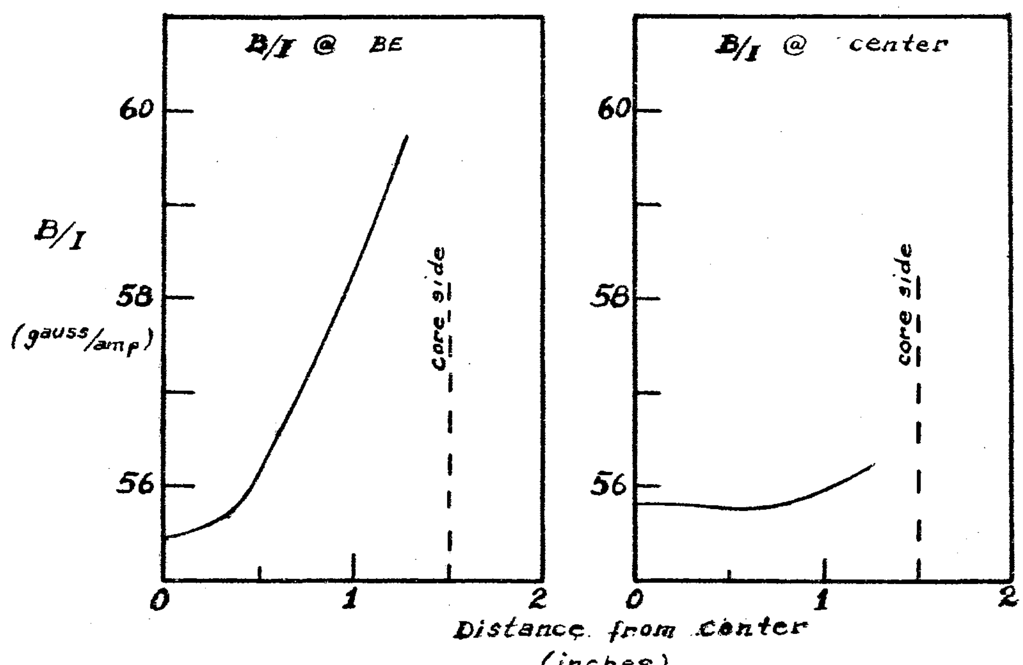

Figure 8. B/I transverse to the coil axis at a position indicated in Fig. 6 and at the center of the coil.

CHAPTER III

CONCENTRIC BUCKING COILS

Before, two identical coils have been used for NMR measurements: one coil for polarization of the sample under study and the subsequent pick-up of the ensuing precession signal and the second coil for picking up superfluous noise which is common to both coils so that with the coils antiparallel this noise signal is cancelled out. For noise bucking by this arrangement the magnetic flux density ideally should be constant in the plane perpendicular to the axis of the coils; if such is not the case, the difference in the average flux for each coil, which induces an e.m.f. with a frequency in the bandpass of the tuned circuit, will appear as noise.

Consider two concentric coils with their axes in the y direction as in Figure 9. The induced voltage in one of the coils is $\mathcal{E} = N\frac{d\bar{\varphi}}{dt}$ where N is the number of turns in the coil and $\bar{\varphi}$ is the average flux enclosed by each turn. This can be rewritten as:

$$\mathcal{E} = N \int \frac{d\vec{B}}{s\,dt} \cdot \vec{n}\, da$$

where $\vec{B}$ is the flux density and

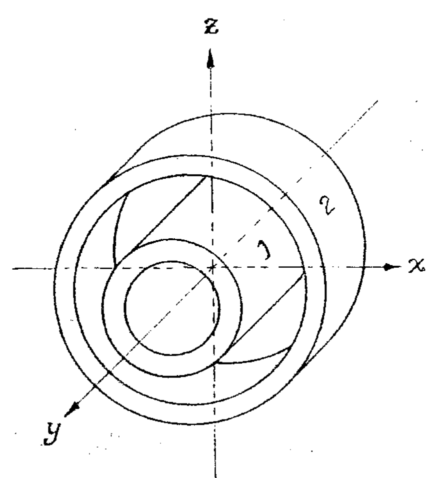

Figure 9. Two Concentric Coils

the integration is performed over an average area enclosed by one turn. If $\bar{B}_y$ is the average y component of the flux density $\vec{B}$, then the expression for induced e.m.f. can be written

$$\mathcal{E} = NA \frac{d\bar{B}_y}{dt}$$

where again A is the average area enclosed by a turn of the coil. If B_y is constant or varies linearly in the x-z plane, then the average flux density for any two concentric circular areas in the x-z plane would be the same. Then the condition $N_1A_1 = N_2A_2$, where the subscripts refer to the two different coils as indicated in the diagram, will insure that the voltages induced in each of the two coils are equal. Another way of stating this condition is that the sum of area enclosed by turns, or the area turns of the two coils, must be equal.

While the variation of the flux density in a plane perpendicular to the axes of two concentric coils may not be linear, to the degree that it is, the noise cancellation will be complete.

It was decided to construct such a pair of coils with the inner one to be identical to those whose design was previously discussed in this paper.

Design of the Concentric Bucking Coil

An expression was developed for the area-turns in a coil so that a large concentric coil could be designed that had the same area-turns as the coil designed previously. Referring to Figure 10 on the following page, $N\frac{dr}{c}$ is the radial density of turns so that the area turns of the coil is given by:

$$\text{Area-turns} = \int_{r_1}^{r_2} \pi r^2 \, N\frac{dr}{c}$$

$$= \frac{\pi N}{3c}\left(r_2^3 - r_1^3\right).$$

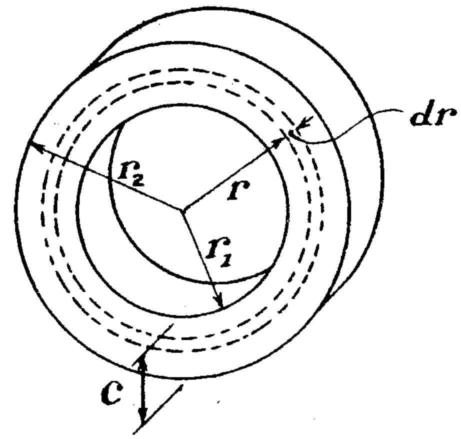

Figure 10. Diagram for area-turns expression.

This quantity was calculated for one of the seven-section coils; once for an end section and once for one of the five small sections, and the results summed so that for the whole coil the area-turns was found to be 1.774×10^4 in^2-turns.

A disadvantage of the concentric bucking coil is that it picks up a portion of the precession signal so that it is somewhat deleted. It was decided that the concentric coil should be of such dimensions that its pickup of the precession signal would be about 3% of that signal strength induced in the inner coil. This is equivalent to the concentric coil having a B/I at its center of about 3% of the B/I of the polarizing coil at the center.

Three concentric coil configurations were considered; a single thin coil, a Helmholtz arrangement of two coils, and a solenoid coil. The first would have to be of rather large diameter to have the required area-turns and the third would limit cooling to some extent of the polarizing coil, so that a Helmholtz configuration was chosen.

For a first approximation in the design the simple formulas

$$B/I = \frac{\mu_0 N}{r} \, \frac{8}{5^{3/2}}$$

for Helmholtz coils and $2N\pi r$ for the area-turns (where N is the number of turns in one coil) were used to plot B/I vs. radius of the coils and B/I vs. the number of turns. From this plot it was found that with N = 42 turns and r equal to about eight inches the B/I at the center for the Helmholtz coils was very nearly that required above.

Using the more exact expression $\frac{N\pi}{3c}(r_2^3 - r_1^3)$ for the area-turns and setting the expression equal to 1.774×10^4 in^2, with N = 84 and selecting c so that it was six layers of 19/27 stranded wire, calculations resulted in r_1 = 8 inches and r_2 = 8.44 inches. The important quantities for the concentric coils were then:

N = 42 turns (one coil only)
L = 0.61 inches (width of one coil)
c = 0.44 inches
r_1 = 8.0 inches
r_2 = 8.44 inches
a = 8.22 inches (center to center separation distance of the two coils).

B/I was then calculated using the more exact expression previously used and was found to be 2.92 gauss/amp, which is 5% of the value for B/I calculated for the polarizing coil.

Two forms cut from a solid piece of phenolic were used for the concentric coils, and winding was done directly on these forms. The wire was 19/27 stranded wire and the coils had each six layers with seven turns per layer. For the inner coil and the outer concentric coils the following measurements were made:

Inner Coil	Helmholtz Coils (two together)
L = 52.0 mh	L = 3.76 mh
R_{dc} = 4.15 ohms	R_{dc} = 1.15 ohms
Q = 148 at 2.3 KHz	Q = 46.5 at 2.3 KHz
f_s = 80 KHz	f_s = 157 KHz

With the three coils together and bucking:

$$\begin{aligned} L &= 51.6 \text{ mh (by imped. bridge)} \\ &= 51.2 \text{ mh (by capacitance required for res. at 2.3 KHz)} \\ Q &= 123 \text{ at 2.3 KHz} \\ f_s &= 74.5 \text{ KHz} \end{aligned}$$

Measurements for Q were made in the same manner as previously described, and these values of L and R_{dc} were made on a General Radio portable impedence bridge.

B/I was determined for the polarizing coil and for the concentric coils on a Bell Model 300 gaussmeter. B was measured for the three coils together, in one case with the fields of the Helmholtz coils and the polarizing coil opposing, and then with the fields adding. The results were B/I for the polarizing coil alone, 58.4 gauss/amp, and for the Helmholtz coils alone, B/I was 2.36 gauss/amp or less than the calculated value by 19%.

Evaluation of Concentric Bucking

In order to accurately compare the improvement of flux noise bucking of the concentric coils over that of the identical coils, ideally noise pickup by both sets of coils would be measured simultaneously with both sets in the same noise environment. Since this was not possible with the equipment that was available it was hoped that some indication of the relative effectiveness of the two sets of coils could be made by measuring their noise pickup separately in the same noise environment.

In the lab each set of coils was tuned to a frequency of 2.3 KHz; their pickup was amplified by a Tektronix model 122 differential preamplifier with a modified bandpass from 800 to 6000 Hz. The measured gain of the amplifier at 2.3 KHz was 680. The noise was then read on a Ballantine true RMS voltmeter model 320A. Since the concentric coils were not inductively symmetrical for provision of a reference point for differential amplification, they were tuned with two identical capacitors in order to provide the required circuit symmetry. Background noise during these measurements was from the fluorescent lights and the electronic equipment.

Noise from each set of coils was measured as a function of their orientation with the coil sets rotated both in a plane perpendicular to their axes and parallel to their axes. Plots are given in Figures 11 and 12 showing the results of these measurements. In the plots with the coils' axes horizontal, the coils' axes were parallel to the fluorescent light bulbs at 0 and 180 degrees. With the coil axes vertical, a signal generator was connected to an inductor and set to radiate at 2.3 KHz. This inductor was at a distance of about twenty feet from the coils. With the radiating coil at this distance it was found that the concentric coils picked up no measureable amount of the 2.3 KHz radiation, and the noise on the plot for the concentric coils is predominantly from the fluorescent lights. All that the results of these measurements in the lab demonstrated was that the concentric coils were built properly; it remained to be seen whether the noise at the outdoor location where NMR measurements are actually made has a sufficient gradient so that the concentric configuration would be beneficial.

With the coils outside, the preamplifier was followed by an output filter with a bandwidth of about 200 Hz centered at 2.3 KHz. This was a different Tektronix 122 preamp and it had a gain of 1200. The preamp output filter consisted of a high Q inductor in series with a capacitor, and the voltage was measured across the inductor, thereby providing an overall system gain of 15,700 at 2300 Hz. Noise was measured with both sets of coils and with the preamplifier input shorted, both at the distant end of the 100 foot cable and at the input of the preamp.

Noise transients were observed with both coil sets; the following values are those recorded during "quiet" periods when the signal from the coils was fairly constant:

		voltage (true RMS)
identical coils	5.5 mv	0.35 microvolts
concentric coils	4.0	0.25 "
cable shorted	2.5	0.16 "
preamp shorted	2.5	0.16 "

The noise due to each coil set is the square root of the difference of the squares of total noise and preamp noise alone; so that for the two coil sets the noise was:

identical coils	0.31 microvolts
concentric coils	0.19 "

The thermal noise for each set of coils was calculated using the expression

$$E(\mathrm{rms}) = (kT\omega X)^{\frac{1}{2}}$$

where k is Boltzmann's constant, T is the absolute temperature in degrees Kelvin, ω is the resonant frequency times 2π and X is the inductive reactance of the coil. From this the thermal noise found for the identical coils was 0.30 microvolts, and for the concentric coils 0.21 microvolts. Therefore only the thermal noise of the coils had been measured. By observing on an oscilloscope transients that occurred, it was not possible to determine whether one set of coils was better than the other in noise bucking.

The period over which these preceding measurements were made was a poor one for the present purposes; the ambient noise was very low.

Only with use under different noise conditions will it be found whether the concentric configuration will prove to be more effective in bucking than the identical coils.

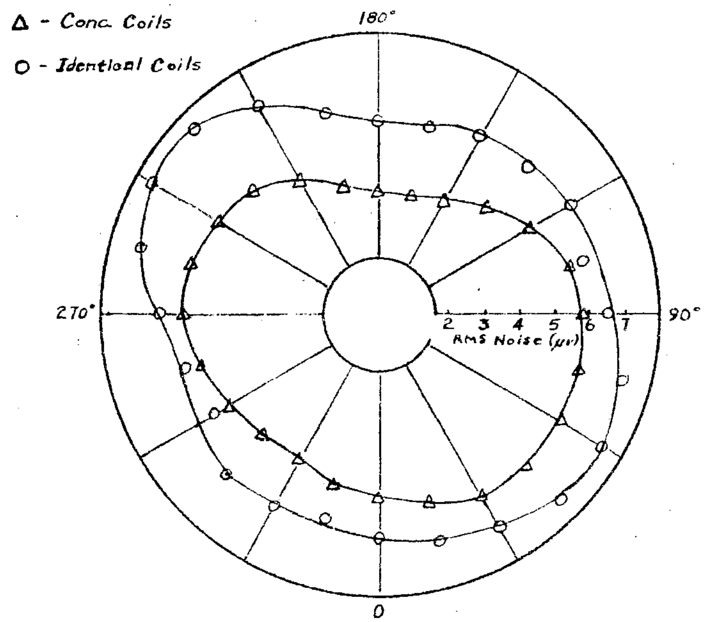

Figure 11. Noise vs. orientation; rotation is in plane of coil axis. Noise includes that due to preamplifier.

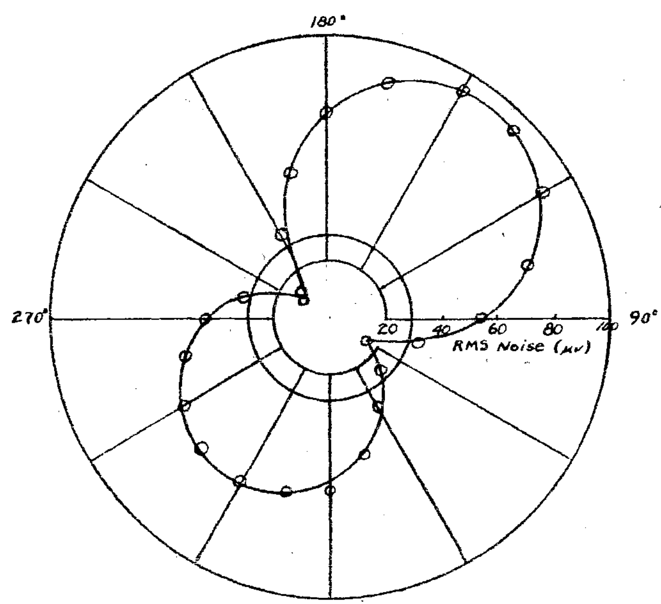

Figure 12. Noise vs. orientation; rotation is in plane perpendicular to coil axis. Pickup by concentric coils is represented by circle at about 30 microvolts.

CHAPTER IV

INTRODUCTION TO PROTON RELAXATION IN MUSCLE

The muscle and in particular the phenomenon of contraction, has in recent years been a subject of intense investigation and much information has been gained in regard to the structure of the agents of contraction as well as the dynamic chemistry of muscle cells. As in any living cell, water plays diverse and important roles in the muscle cell or fiber. The role water plays in the actual process of contraction is also with little doubt diverse and important.

In the skeletal muscle of man the water content of a wet muscle, that is as it is found in the body, is nominally 80% by weight and around 80% of this water is intracellular. The remaining extracellular water, the interstitial or tissue fluid, is in composition similar to blood but distinguished from it by the absence of the blood cells and some of the larger molecules found in the blood. Additional blood volume in the muscle is about one-third that of the interstitial fluid. The interstitial fluid is a homogeneous aqueous solution, while in contrast, the fluid inside the muscle fibers, due to the semipermeable properties of the fiber's membrane and the internal structure of the cell, may be considered a multi-phased medium.

The remaining portion of the muscle is largely protein. In a single muscle fiber are many fine fibers of about one micron diameter which are called myofibrils. These myofibrils, which are the actual contractile structures, are composed primarily of the proteins myosin and actin. This then is a very general picture of the environments in which a water molecule in muscle may find itself: in a homogeneous phase outside of the muscle fibers; inside the cell in an inhomogeneous phase, the water molecules influenced more or less strongly by association with protein. The bulk of this protein is in structures which play a direct or indirect role in the primary function of the cell, namely contraction.

Bratton, et al., using a skeletal muscle of a frog, found that at fields corresponding to Larmor frequencies of 24.0 MHz and 4.30 MHz, T_1 was 400 msec at the larger field and 250 msec at the smaller. T_1 appeared to be independent of the state of the muscle while T_2 was the same at the two field strengths and increased with tetanic isometric contraction from 40 msec for relaxed muscle to 60 msec with exhaustion of the muscle. These results did not permit a homogeneous phase for the water, and three models were suggested that might account for them. That most attractive on the basis of their work was a two phase model for water in the muscle cells, the exchange rate of water molecules between the two phases being sufficiently great that unique effective transverse and longitudinal relaxation rates were observed. These two phases were termed liquid and solid-like, the former being characterized by a correlation time τ_1, and the phase of water with restricted rotational freedom by τ_2. These correlation times were considered to meet the condition

$$\tau_1 \ll \frac{2\pi}{\omega} \ll \tau_2$$

where $\frac{\omega}{2\pi}$ is the Larmor frequency. In the limiting case of fast exchange, the total magnetization of the sample decays toward equilibrium with a time constant T^{obs}, where

$$\frac{1}{T^{obs}} = \frac{1-f}{T^{(1)}} + \frac{f}{T^{(2)}} \qquad (1)$$

where the superscripts 1 and 2 refer to the two phases whose correlation times were previously so designated. f is that fraction of the water in the solid-like phase and (1-f) is that fraction liquid. The general expressions for the relaxation rates for intramolecular proton-proton dipole interaction in a liquid such as water having two protons per molecule are:

$$\frac{1}{T_1} = K\tau_c \left[\frac{1}{1+\omega^2\tau_c^{\,2}} + \frac{4}{1+4\omega^2\tau_c^{\,2}}\right] \qquad (2)$$

$$\frac{1}{T_2} = K\tau_c \left[\frac{3}{2} + \frac{5/2}{1+\omega^2\tau_c^{\,2}} + \frac{1}{1+4\omega^2\tau_c^{\,2}}\right] \qquad (3)$$

where $K = \frac{3}{2}\frac{\hbar^2\gamma^2}{b^2}$; γ is the gyromagnetic ratio of the proton and b is the proton separation distance on a water molecule. Applying the condition imposed on the correlation times of the two phases and combining the resulting equations for the effective relaxation rates observed results in the rate equations used by the authors:

$$\frac{1}{T_1} = 5(1-f)K_1\tau_1 + fK_2\tau_2 \left[\frac{1}{1+\omega^2\tau_2^{\,2}} + \frac{4}{1+4\omega^2\tau_c^{\,2}}\right]$$

$$\frac{1}{T_2} = 5(1-f)K_1\tau_1 + \frac{3}{2}fK_2\tau_2$$

where the authors differentiate between the constants K_1 and K_2 for the two phases. With the substitution of their data into the rate equations,

$\tau_2 = 1.6 \times 10^{-7}$ sec and $fk_2 = 9.42 \times 10^7$ sec^{-2} and the product $5(1-f)k_1\tau_1$ is 2.39 sec. Making the further assumption that rather than being given by eq. (3) above, T_2 may have reached its asymtotic value, they go on to predict a range of possible values for f of from 4.5×10^{-6} to 1.5×10^{-3}, the latter which they favor, corresponding to the interaction strength of water protons in ice. It is pointed out that in the transverse relaxation rate equation the solid phase contribution is dominant over that due to the liquid phase so that with contraction, a decrease by 20% in the fraction f would account for the observed muscle-state dependence; this situation would account also for the field independence of T_2. Conversely, the liquid phase dominance of the longitudinal relaxation rate would result in the apparent muscle-state independence and the field dependence observed for T_1.

The work carried out and described in the following pages was intended to determine whenter useful measurements on muscle could be made using as convenient a sample as the human arm with low-field NMR apparatus, and if so to further investigate the relaxation rates over a much broader, though lower, range of fields. Furthermore, it was hoped that the adequacy of the model proposed by Bratton, Hopkins and Weinberg could be tested.

CHAPTER V

THE EXPERIMENT

With the low field NMR equipment used it is possible to measure longitudinal relaxation rates in fields from one gauss up to about 390 gauss in increments corresponding to fifteen different field strengths. This range in Larmor precession frequency for protons is from 4.26 KHz to 1.66 MHz. The transverse relaxation rate can be measured only in the earth's field, that is at a Larmor frequency of 2.3 KHz.

The coils used for polarization of the sample and pickup of the ensuing precession signal were those described in the first section of this thesis, the polarizing and bucking coils being those identical to each other. The core diameter of these coils is three inches, and the length is 8.2 inches. It seemed most desirable to have a subject's upper arm in the coil rather than the forearm because of the larger sample volume of muscle afforded. However there was some difficulty in finding upper arms meeting the dimensional requirements imposed by the coil. Of the four people who served as subjects, forearm measurements only were made on two.

Anatomy of the Arm

A general survey of arm anatomy is necessary in view of the fact that water occurs in a variety of tissues and structures in the arm and any signal received from proton precession in the arm will be a composite signal, the components of which are not all of interest here. The major tissues found in the arm are muscle; the fascia which is itself a membrane that jackets each individual muscle but which is associated with fat that cushions the muscle; the skin and its associated underlying fat; the marrow of the bone; the connective tissues; and the blood.

In the forearm are found nineteen different muscles which are divided up in two major groupings: the flexors and the extensors. The muscles of the flexor group are located mostly on the anterior side of the forearm, that is on the side of the palm, and as indicated by the name of this grouping, they are responsible primarily for gripping action. The extensor muscles, which among other things extend the fingers, lie primarily on the posterior side of the arm. Some muscles in both of these groups are responsible for the many movements of which the wrist and forearm are capable. Most of these forearm muscles taper off rapidly toward the hand and a few inches above the wrist are replaced by tendons that pass on through the wrist making their insertion attachment in the hand. For the present purpose this situation is important in several respects: 1) there are so many muscles that the fascia and the fat surrounding each muscle represents quite a portion of the volume of the arm which might normally be thought of as solid muscle 2) tendons comprise a sizeable portion of the forearm 3) attempting to tense all muscle to a fair degree simultaneously might be a problem, although making the arm tensely rigid seems to involve all the muscles of the arm.

The fraction of the total arm volume represented by each different tissue will vary from individual to individual. The arm of one of the earlier subjects was x-rayed and the volume of that portion of his arm in the coil was measured by water displacement. With this information an attempt was made to determine the volume of each of the major components of the arm, and in particular the volume of the muscles. On the x-ray, which was taken in two orthographic views, two boundaries could be distinguished: that between the bone and the surrounding tissue, and that between the fascia which encases all the muscles together and the fatty tissue underlying the skin.

The volume of the forearm in the coil was found to be 557 ml. The volume of bone, the skin and underlying fat, and the muscle, which here is taken to be everything but the other two components, was found to be as follows:

	volume	%
skin and fat	142 ml	26
bone	47 ml	8
muscle	368 ml	66
total	557 ml	100

This volume of a segment of the arm cited above is less than was in the wound length of the coil. In the first section of this thesis a plot of the axial field to current ratio for this coil was given (see Figure 7). Since the axial field decreases rapidly along the last inch of either end of the coil, the effective sample length was considered to be from midpoint to midpoint of the coil's end sections.

The volume of muscle itself is probably about 60% of the total volume, or 344 ml. Of this volume, water is about 80% or 267 ml. As was mentioned earlier, part of this water is intracellular and part extracellular. The water in the muscle can then be broken down as follows:

total water in muscle	267 ml
water in the muscle cells	214 ml
water in muscle but not in cells	53 ml

In addition to the intersititial fluid there would be some 18 ml of blood in the muscle.

The anatomy in the upper arm is much simpler than that in the fore-arm; there are five muscles divided into flexor and extensor groups, the action of which is at the elbow and the shoulder joint. The tendons connecting these muscles to bone are quite short. From the x-rays of the upper arm of the same subject as above:

	volume	%
skin and fatty tissue	218 ml.	26
bone	42 ml.	5
muscle	580 ml.	69
total	840 ml.	100

Using the same distribution of water in the muscle and assuming that 65% of the total volume is muscle rather than the 69% calculated from the x-ray:

total water in muscle	437 ml.
water in the muscle cells	328 ml.
water in muscle but not in cells	109 ml.

The upper arm of this subject was slightly too large for the coil, but the preceding figures indicate the relative muscle water in these two portions of the arm. The ratio of muscle water, or muscle volume in the upper arm to that in the forearm is 1.63 to 1. It was hoped that results of the preceding considerations would not be far wrong for any of the subjects used in the experiments since their arms were of similarly lean proportions.

It should be pointed out that although the muscle is only about 2/3 of the volume of these two segments of the arm, the muscle water actually accounts for a much larger portion of the total water in the arm segments. This is so because fatty tissues contain relatively little water.

The subject, seated beside the coils, with one arm in the polarizing coil, was grounded in common with the electronic equipment to minimize noise. It was found that the subject could have one arm in each coil and not be grounded or one arm in and be grounded with no difference in the noise. The latter arrangement was used for greater comfort of the subject.

The Measurements

In order to measure T_1 over a range of field strengths down to one gauss, two different experiments are required. The first, which will here be referred to as experiment #1, involves polarizing the sample for a variable length of time and observing the relative signal strength for each of these periods of polarizing. The second, for low fields, involves polarization of the sample for a sufficient length of time that the sample is fully polarized; then the polarizing current is reduced so that relaxation occurs in the smaller field with a time constant T_1. This "pedestal" experiment will be refered to here as experiment #2. The magnetization diagrams on the following page illustrate the above.

The amplitude of the signal induced in the coils by the precessing magnetic moments of protons is proportional to the magnetization, and after amplification what is actually observed with an oscilloscope is a 2.3 KHz signal decaying with a time constant T_2 representing the decay of the magnetization in the earth's field. T_2 decay curves, as on the diagrams, are then directly observed. In experiment #1, at time t, and in experiment #2 at time $t_p + t$, the sweep rate of the oscilloscope is

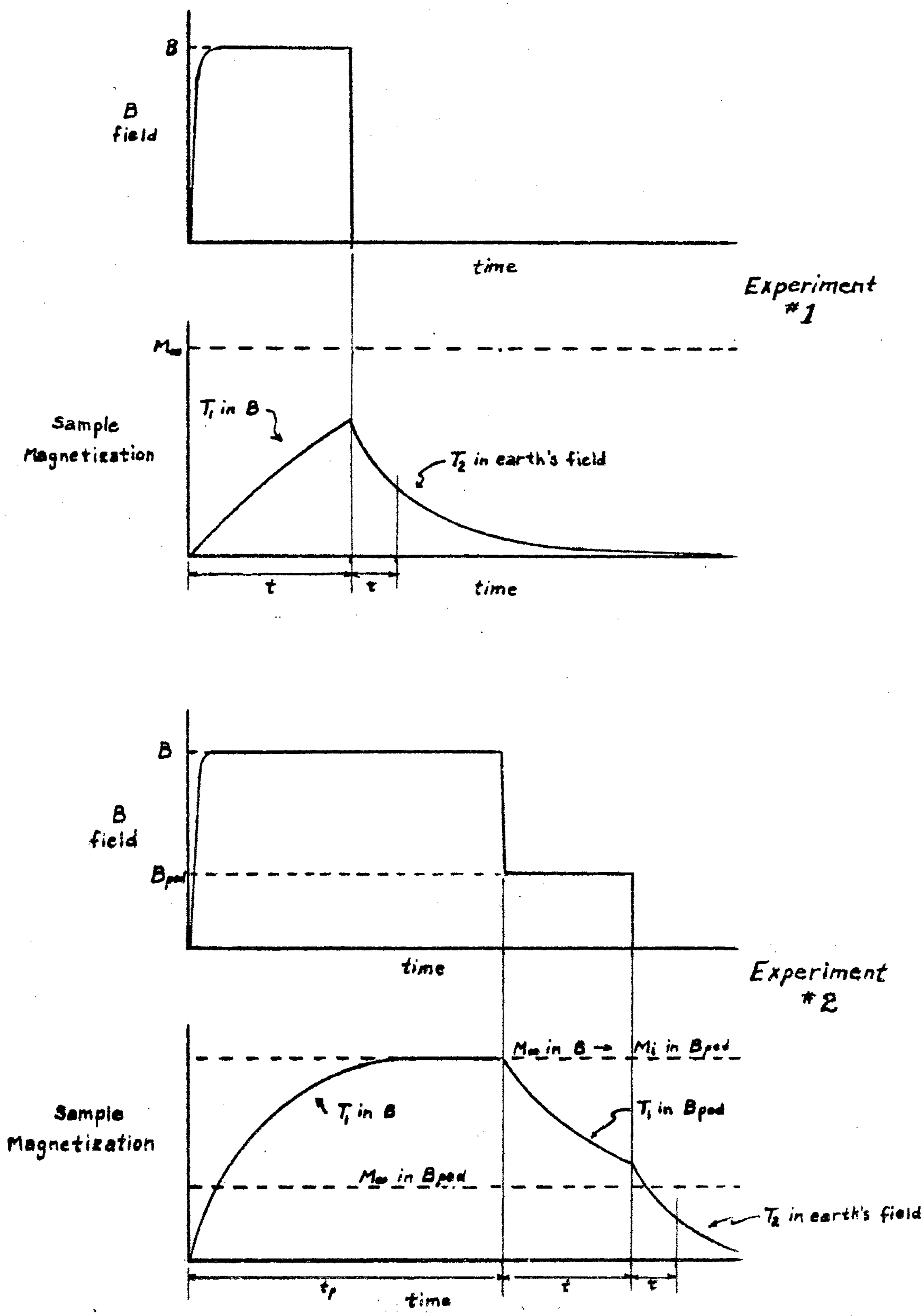

Figure 13. Diagrams illustrating experiments 1 and 2.

triggered; but due to the "ringing" of the coils at precession frequency it is not until a time τ, as indicated on the diagrams, that the desired signal can actually be measured. By varying the polarization time t, or the pedestal duration t, all the resulting signal amplitudes observed at time $t + \tau$, when plotted against t, give the exponential magnetization curve with time constrant T_1 for the sample in the field B or B_{ped} according to the experiment. As long as τ is constant it can be neglected for the purpose of finding T_1. The time τ is about 100 msec when using the full Q of the coils. When a resistor is placed in parallel with the coils to lower their Q to about 25, τ is around 45 msec. If T_2 is on the order of 50 msec for the water in muscle, the the major portion of the decay signal will be lost before it can be observed.

If the amplitude of the signal is E(t) at time t, then for experiment #1:

$$E(t) = E_\infty(1-e^{-t/T_1}) \qquad (1)$$

and for experiment #2:

$$E(t) = E_\infty + (E_i - E_\infty)e^{-t/T_1}. \qquad (2)$$

E_∞ can be found in experiment #1, and in experiment #2 for the larger pedestals, by letting $t \gg T_1$. Since by Curie's law M_∞ , the full magnetization, is directly proportional to the field strength, and therefore to the current, then

$$\frac{E_{\infty_1}}{E_{\infty_2}} = \frac{I_1}{I_2} \quad .$$

So long as the pedestal currents are known only one E_∞, either from experiment #1 or from high pedestals in experiment #2, need be measured. Rearranging equations (1) and (2) and taking the log of each side:

$$\ln\left[\frac{E_\infty - E(t)}{E_\infty}\right] = -t/T_1 \qquad (3)$$

for experiment #1, and for experiment #2:

$$\ln\left[\frac{E(t) - E_\infty}{E_i - E_\infty}\right] = -t/T_1 \; . \qquad (4)$$

Each of these equations for two different times, t_1 and t_2, are subtracted from each other resulting in the final expressions from which T_1 is found:

$$T_1 = \frac{t_2 - t_1}{\ln\left(\frac{E_\infty - E(t_1)}{E_\infty - E(t_2)}\right)} \qquad (5)$$

for experiment #1, and

$$T_1 = \frac{t_2 - t_1}{\ln\left(\frac{E(t_1) - E_\infty}{E(t_2) - E_\infty}\right)} \qquad (6)$$

for experiment #2. In experiment #1 the log of $E_\infty - E(t)$ is plotted against t, and from the slope of the line T_1 is found. In experiment #2 log $E(t) - E_\infty$ is plotted against t.

CHAPTER VI

THE RESULTS OF FOREARM MEASUREMENTS

The first subject was male, twenty years of age, of lean proportions and with a muscle tone which was probably average for his age. This subject was available for only a short period of time, and unfortunately the weather was typified by electrical storms and damp ground resulting in rather poor noise conditions. The second subject, for whom the arm water calculations in a previous section were made, was a sixteen year old male. His arm muscles were somewhat "softer" than the first subject's, being probably typical for a boy in early puberty. Over the three week period that measurements were made on this subject the noise conditions were better than previously, and in addition to measurements on the field dependence of T_1, and T_2 measurements in the earth's field, attempts were made to determine the amount of water in his arm from the precession signal.

The results for T_1 field dependence for the two subjects appear to agree well, although there is a good deal of scatter in the data. Figure 14 is a plot of T_1 vs. field for both subjects. Some anomalies appeared in the first set of data taken. T_2 in the earth's field was found to be about 40 msec, in good agreement with that found by Bratton, et al. (1965). However in the dozens of times in which T_2 data was later taken, no value for T_2 was ever measured that was less than twice this. It is possible

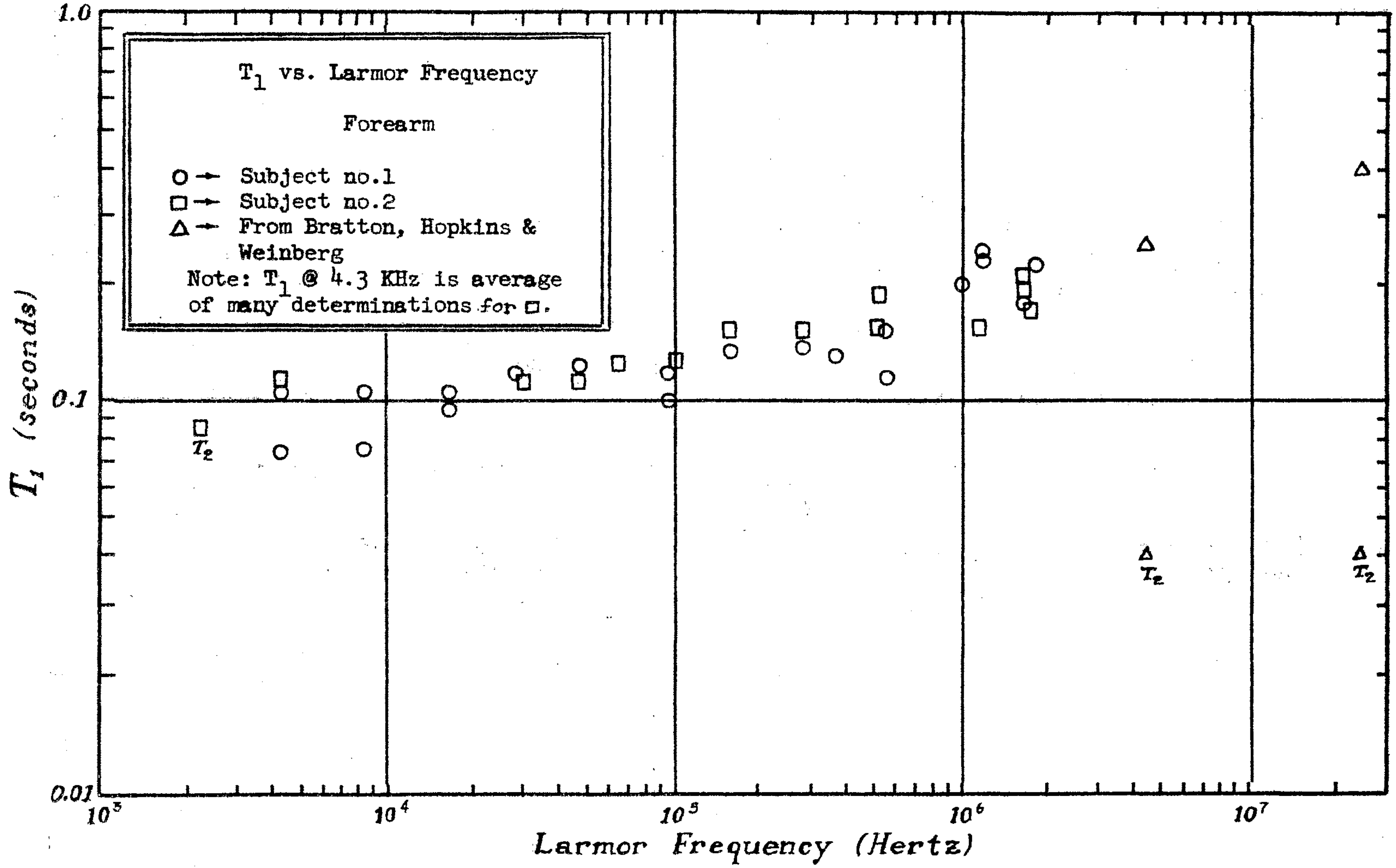

Figure 14. T_1 versus the Larmor precession frequency; forearm measurements.

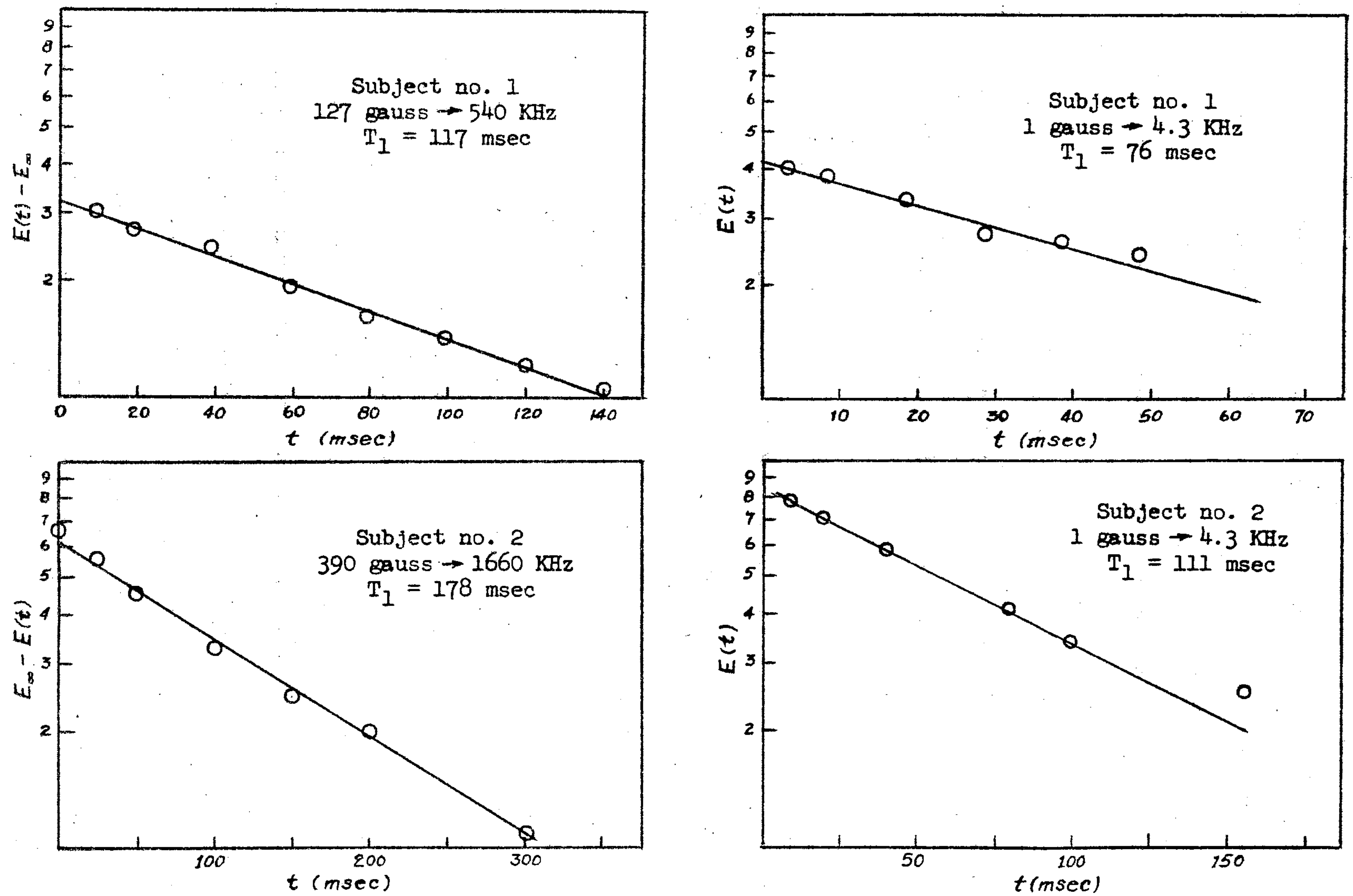

Figure 15. Some typical T_1 data from the forearms of subjects 1 and 2.

that an error was made in recording the oscilloscope sweep rate, though a careful examination of the original raw data seems to rule this out. Conceivably a ferromagnetic object on the subject's person dehomogenized the earth's field, and resulted in a spuriously low measurement of T_2. Other results from measurements on the first subject which stand out from the same measurements on the other three people are unusually low values for T_1 at low fields. A possible explanation for this will become apparent in the discussion of the data from the last two subjects. In Figure 15 are some typical plots of data for T_1 from subjects 1 and 2.

It should be mentioned in regard to sample T_1 data plots that for experiment #1 data, the points on either end of the time scale are considered the least reliable because when t is small the data points are the difference of E_∞ and the smallest $E(t)$, which is that with the poorest S/N ratio; the points at long t are the difference of two large numbers so that any error in one or both of these signal amplitudes is exaggerated in their difference. In experiment #2, the points at short t's are considered the most reliable and those at long t's the least because of the decreasing S/N ratio with longer pedestal duration.

In the T_1 data plots it often was the case that the points at the shorter and longer t's lay above the apparent best straight line. On the premise that perhaps the curve actually was nonexponential due to two separate components, experiments were undertaken that would hopefully exaggerate the two components if indeed they did exist.

It was first thought that if there were two components, the shorter one would have a T_1 around 100 msec while the longer T_1 would perhaps be on the order of a second. T_1 was measured at 120 gauss and one gauss with polarizing times of 500 msec, 1 sec, and 10 sec. With the short polarizing time there would be proportionally more of the short T_1 component present in the initial magnetization for the lower fields, and with the long polarizing time surely both components would have reached full magnetization before they began their decay into the 120 and 1 gauss fields. Also the pedestal time duration was taken out to longer times than had previously been used. These efforts failed to exaggerate any separate components; in fact, the data looked very much like that which had been gotten all along. Similarly T_2 was measured with different polarizing times and similarly the results were negative in aiding in resolution of two separate components. The data was in general good, and it was concluded at this point that either the relaxation is actually exponential or the two components have relaxation times which are much more nearly equal than had been supposed. It should be remembered that because of the time lag between the pedestal cut-off and when the precession signal is actually seen, the amplitude of a signal with a short T_2 will be greatly reduced from its initial amplitude at pedestal cut-off. More will be said about this matter when the data from the upper arms of the last two subjects is discussed.

Measurements were made on the second subject to determine the arm water volume from the precession signal so that this could be compared to that calculated from the x-rays. Two different approaches were made. First the signal amplitude from the forearm was compared to that from a known volume of water. Second, T_1 and T_2 data was taken on the forearm alone and then with the forearm and a sample of water both in the coil. Particularly the first method depends on the linearity of the preamplifier for signals of very different amplitudes. This was checked and found to be quite good. Also the field over the volume of samples to be compared must be uniform; for the signal received from a unit volume of the sample is proportional to the average value of the axial field component for that volume element. Although this condition could only be met for samples of identical size and shape, the error in the methods used was felt to be sufficiently small for present purposes.[1]

In the first method, T_2 for (tap) water was found to be 1.45 seconds, and the maximum signal received from the water with long polarizing time was 2.58 volts, peak value. The average value for T_2 was found for the forearm of this subject to be 87 msec. The maximum signal from the arm was 0.84 volt when the T_1 data from experiment #2 is extrapolated back to t = 0. Volume of the water sample was 200 ml, so that correcting for a time lag of 100 msec after coil current cut-off, the volume of arm water in the forearm segment is:

$$\frac{(0.84)\ \exp\ (100/87)}{(2.58)\ \exp\ (100/1450)} \times (200\ \text{ml}) = 194\ \text{ml}$$

The calculated water in the arm segment was 267 ml, total. The water calculated to be in the muscle cells themselves for this subject was 200 ml; however the signal for all the water should have been what was measured, not just the intracellular water. If the data is not exponential with one component too short to resolve, then of course there was error in extrapolating the arm T_1 data back to t = 0 pedestal dura-

[1]See plots of the axial field to current ratio for these coils, page 22.

tion, as well as in the correction for the 100 msec time lag. Non-exponential relaxation may therefore be responsible for the discrepancy between the estimated water volume of 267 ml and the measured volume of 194 ml. Another possibility is that with the arm in the coil the Q of the coil was lowered, reducing the observed signal in proportion to Q. It was hoped that the second method would avoid the latter possibility.

Small samples of water were placed in plastic bags for the second method of arm water volume determination. The two sets of T_1 data using experiment #1, one of the arm alone and one with arm plus water, were plotted on the same semilog paper and extrapolated back to $t = 0$. The two curves were then subtracted from each other to give a T_1 curve for water alone. This was done on two different occasions, the first time with 25 ml of water and the second time, on a different day, with 50 ml of water. The curves from both of these sessions are shown in Figure 16. The signal amplitude for the water alone at $t = 0$ when the two curves are subtracted one from the other does not agree with the signal amplitude measured for the water samples alone in the coil. This is indicated in Figure 16 . If the difference of the two T_1 curves is taken as that due to the water sample alone, then the arm water volumes, when corrected for the dead time, are 260 ml and 244 ml respectively for the 50 ml and 25 ml tap water experiments. If the independently measured water sample amplitudes are used with the T_1 intercept at $t = 0$ for the arm alone, as was done in the first method, then the volumes of arm water are found to be 195 ml and 208 ml for the 50 ml and 25 ml experiments respectively, in good agreement with the first method, above. The discrepancy between the two methods may be accounted for by the

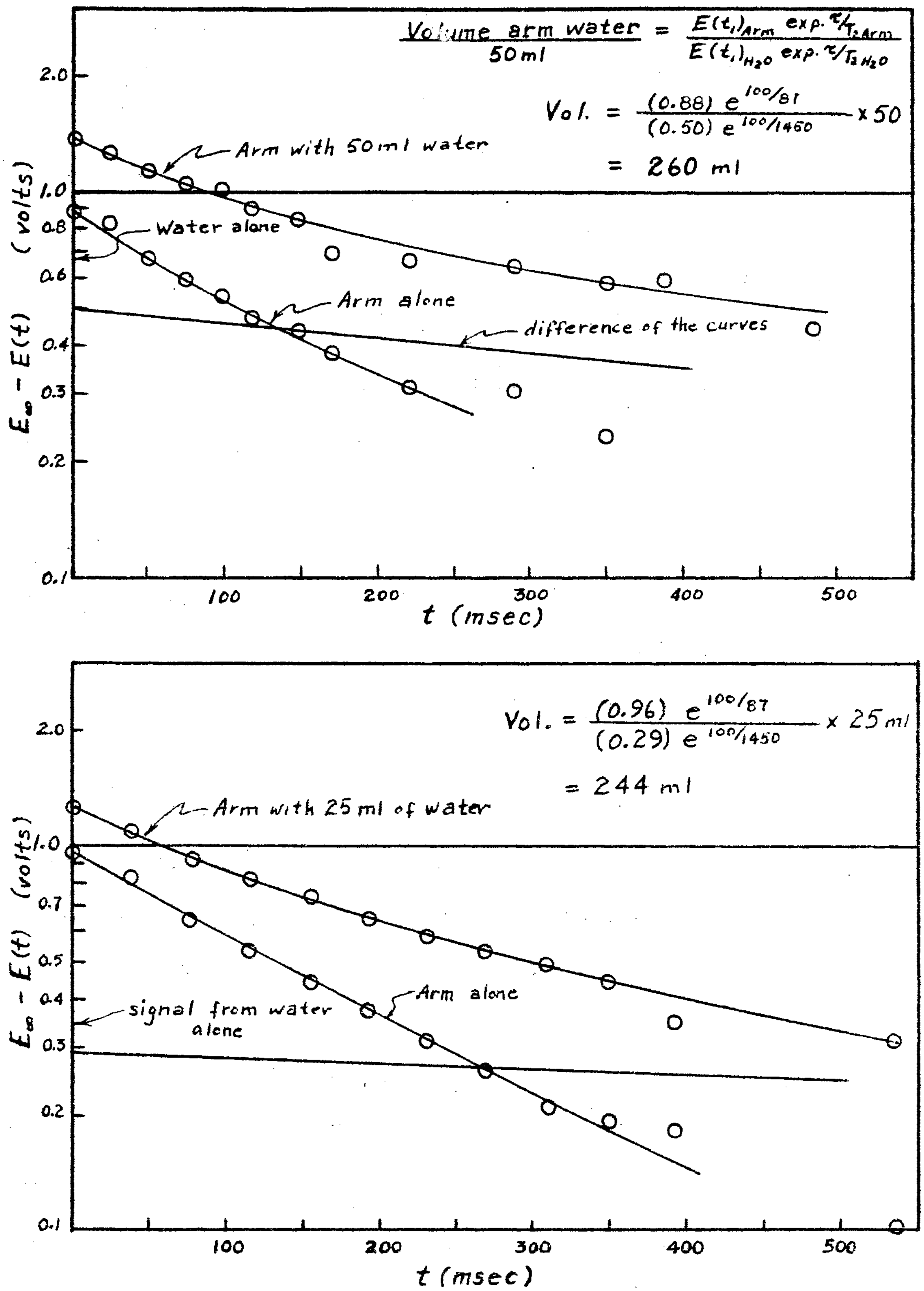

Figure 16. T_1 data from experiment no. 1 for determination of forearm water volume (see text).

presence of the arm and arm plus water lowering the Q of the coils so that the gain of the system was less when an arm was in a coil than when measurements were made on the water sample alone. If this is the case then the figures for the arm water volume are 260 ml and 244 ml, which agree reasonably well with the 267 ml calculated from the x-rays. Q of the coils with and without an arm had been measured much earlier and found to be essentially the same, but this would not rule out the possibility that the coils had since become more lossy. With use the film insulation of the coil wire strands in the core wear down and there could have been some condensed moisture on the plastic water bag and perspiration from the arm. A partly shorted turn could result in a substantial decrease in Q.

Up to now little has been said about the results of T_2 measurements other than that found for subject #1 was an odd value. Many T_2 determinations were made on subject #2. T_2 data was taken over a range of 100 msec, that is from the interval from 100 msec to 200 msec after coil current cut-off. The average value for all the determinations is 87 msec, though the best data, that with practically no scatter, gives a value for T_2 in the earth's field closer to 90 msec.

CHAPTER VII

UPPER ARM MEASUREMENTS

The third subject was a thirteen year old boy. His upper arm fit somewhat loosely in the coil; it was about 8.5 inches in circumference, filling about 87% of the available coil core volume. The fourth subject was a woman fifty-nine years of age. Her upper arm made a tight fit in the coil providing a larger sample volume than any of the previous people. In general the arm makeup of both of these last two subjects differed from the earlier subjects in that there was an appreciable layer of fat on their arms.

The reason that the results of measurements on the upper arms are presented separately is that the signal to noise for this data was improved, and the primary T_1 and T_2 relaxation was found to be nonexponential. As was previously discussed, the data from the forearm appeared to be perhaps nonexponential, but as a rule the scatter in the data was too great to be certain of this. That T_2 data, as well as T_1 data, was nonexponential became definitely apparent when the precession signal was plotted out over the interval from 50 to 200 msec instead of the 100 to 200 msec interval that had before been used for T_2 determination. Failure to take into account this systematic curvature in the forearm data from which T_1 and T_2 were extracted perhaps accounts partially for the rather large scatter in the T_1 field dependence plot for the first two subjects.

The most obvious explanation for the nonexponential data is that what is being seen is the sum of two or more separately decaying exponential signals. This would require two or more environments for protons in the arm between which the exchange rate of water molecules is negligibly low. Bratton, et al., assume for their model that there are two phases with a sufficiently fast exchange rate that the relaxation of the muscle water protons is effectively exponential. A third possibility is that exchange between the environments is at an intermediate rate so that neither of these extreme situations is applicable. In order to discover which of the two possible explanations for the nonexponential nature of the T_1 and T_2 data is correct, the following analysis of the data was made. The data used was from the fourth subject because she was available for measurements over a long period of time.

T_2 data was broken up into two components and these extrapolated back to $t = 0$. The two intercepts should represent the relative water volume for each of the environments, and if the relative volumes cannot be accounted for on anatomical grounds then this would indicate intermediate exchange. In Figure 17, T_2 data is plotted out to 200 msec; the two components are shown extrapolated back to $t = 0$. There is a good deal of arbitrariness involved in drawing the long time tangent, and any error is exaggerated in the resulting short time component. From a number of reasonable tangents drawn it does appear, though, that the two components are about equal, so they are assumed to be so. Comparing signal amplitude from a known volume of water, the sum of the components requires a water volume of 560 ml and therefore a water volume

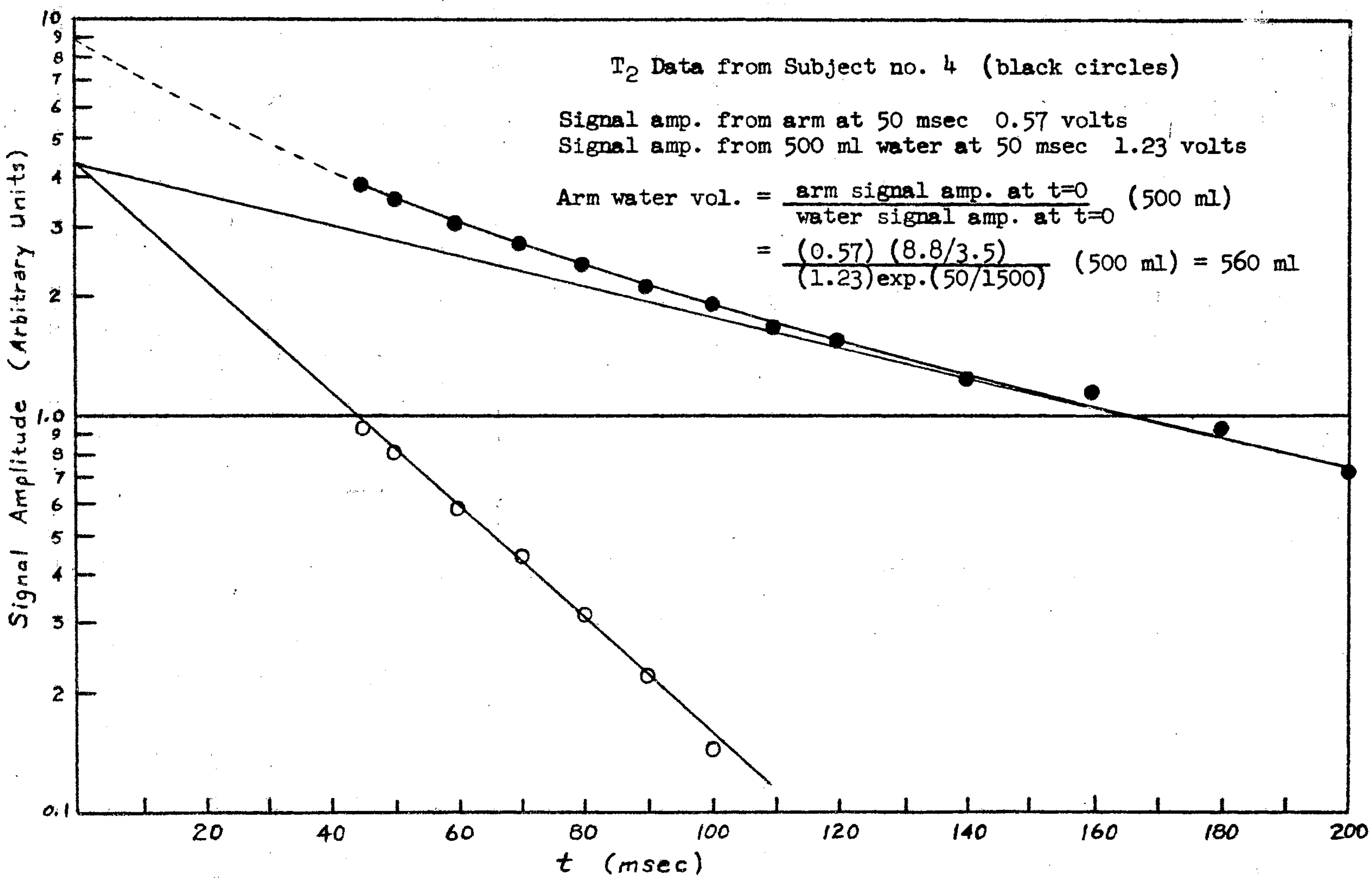

Figure 17. Component analysis of T_2 data for arm water volume determination.

for each environment of 280 ml.

The thickness of the skin and the underlying fatty tissue of this subject was estimated by "pinching" her arm; it appeared to be about 3/8 of an inch thick on the average, being much thicker on the under side of the arm than on the top. Taking the arm diameter to be three inches, the same as that of the coil core, and considering the bone to comprise 5% of the total arm segment volume, as was found for the subject whose arm was x-rayed, the volume of the arm breaks down as follows:

skin and underlying fatty tissue	350 ml
muscle (including inner fascia and fat)	450 ml
bone	40 ml

If the volume exclusive of the bone and the skin and underlying fat is taken to be entirely muscle, then the water in the muscle would be 360 ml, or 80% of the muscle volume. Since the water content of adipose or fatty tissue is negligibly low and the signal amplitude from the arm corresponded to a water volume of 560 ml, not only can two separate but equal components not be accounted for anatomically, but even the total signal amplitude measured cannot be explained.

Independent measurements were made on pork fat tissue. Any appreciable signal from such a sample must be accounted for as being due to the protons of molecules comprising the fat, since the substance fat comprises some 95% of adipose tissue. The results of these measurements on fat were a T_2 in the earth's field of 47 msec and an extrapolated signal amplitude, when compared to that from a known volume of water, corresponding to an equivalent water content of fat of 57%. Applying these results to the makeup of the fourth subject's arm:

fat volume	350 ml
equivalent water volume for fat	200 ml
total water in muscle	360 ml
sum (total equivalent volume contributing to signal)	560 ml

Exact agreement between the expected water volume from the signal amplitude and the estimated equivalent water volume is certainly a coincidence, but the fact that there is agreement between the two figures is interesting. The relative amplitudes for the two components, however, remain to be explained. If the thickness of fat under the skin was one-half inch, the expected results for equivalent water volume would be those found, but this large an error in estimating the fat thickness is unlikely. It is a physiological characteristic of older people that there is a good deal of fat accumulation throughout the body regardless of whether or not the person appears obese. The above results could well be accounted for by the large fat volume required by the signal amplitude being distributed throughout the muscle, that is thick adipose layers associated with all fascia in the arm,at the expense of muscle volume. If in this arm segment there was 490 ml of adipose tissue and 350 ml of muscle, the results would be about those found from the measurements.

On the basis of the above it is tempting to assign the short component from the T_1 as well as the T_2 data as being due to fat, and the long time component as being due to water in the muscle. This would further explain why the nonexponential character of the data was difficult to detect from the forearm measurements since the two subjects used were lean young men. However, earlier T_1 and T_2 data had been taken on beef fat, and although the data was not of good quality due to the low signal, these measurements gave a T_2 in the earth's field of 77 msec and a T_1 at one gauss of about 100 msec. The beef fat was very hard and unlike that in texture expected in an arm. It remains to be seen whether the fat with which we are concerned is better represented in composition by the beef or the pork fat samples used. Certainly before definite conclusions can be drawn this matter needs to be further investigated. It can safely be concluded from the signal amplitude that there is not a third component of very short time constant that the effective dead time renders undetectable.

The problem then arose of how best to describe the T_1 and T_2 data so that a meaningful T_1 field dependence could be shown. It was decided that for the purpose of later analysis it might be desirable to describe the data as fully as possible by showing both the field dependence of T_1 for the two separate components and the field dependence of the limiting slopes from the data. Therefore the analysis of the data was made in the following ways:

1. If there were two proton populations with no exchange, the data would properly be described by the two separate components. The field dependence of these components is shown in Figure 18.

2. In order to further describe the actual data taken, time constants corresponding to two tangents to the data curves are given in Figure 19. The line drawn tangent to the curve at $t = 0$ gives what is here referred to as T_1 in the short time limit, and the other tangent gives the corresponding T_1 in the long time limit. The latter is, of course, the same as the long component in Figure 18.

3. If there was sufficiently fast exchange between the proton populations, the T_1 data would be linear on semilog paper. Therefore a

"best" straight line was drawn through the data. In order to minimize the arbitrariness of deciding what the "best" straight line is, the line used was drawn through the amplitude points at t = 0 and t = 200 msec. The resulting line has about the slope that in most cases a line drawn through the most points would have. This line is approximately parallel to a tangent of the data curve at the point of maximum curvature. T_1 field dependence with this analysis of the data is shown in Figure 20. This should appear most like that from the forearm measurements. In Figure 21 are typical T_1 data plots for two different fields along with the graphical manipulations performed on them. A similar analysis of T_2 data was performed.

Measurements of Proton Relaxation in Blood

T_1 and T_2 measurements were made on cow blood in the hope that the results would in some way shed some light on the previous arm measurements. The sample was 500 ml of cow blood taken from a freshly slaughtered animal. As soon as the sample bottle was filled it was sealed and within a period of about twenty minutes measurements were begun on the sample. The T_1 and T_2 data was to all appearances exponential. The field dependence of T_1 along with the earth's field value for T_2 are shown in Figure 22. After several weeks of refrigeration, measurements were again made on this sample. T_1 was measured at only three fields, but this indicated that the field dependence was essentially the same as it was for the fresh blood with the T_1 curve in the low fields shifted up in T_1 by about 30 msec.

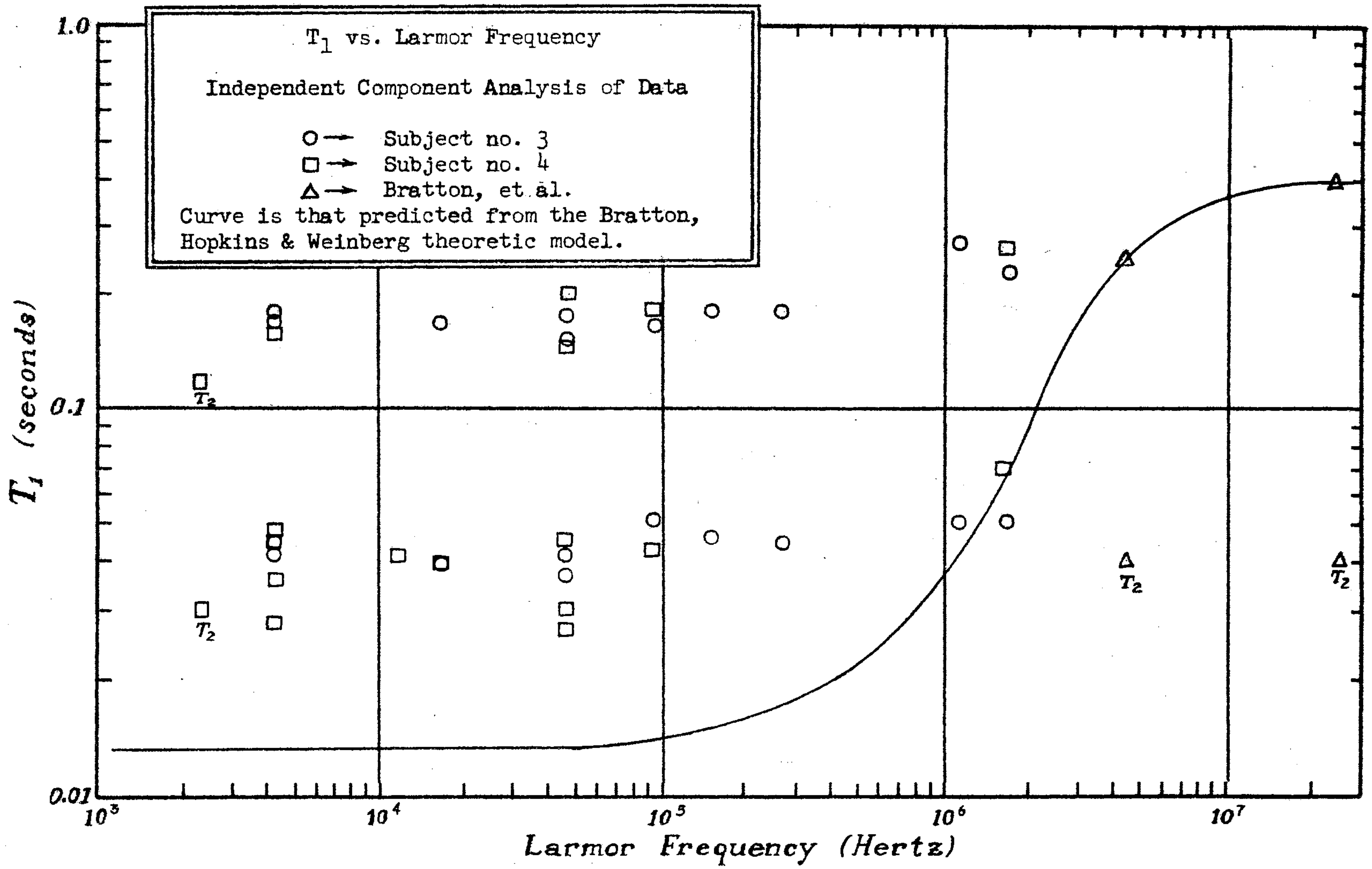

Figure 18. T_1 versus the Larmor precession frequency; data was considered to be the sum of two independent precession signals.

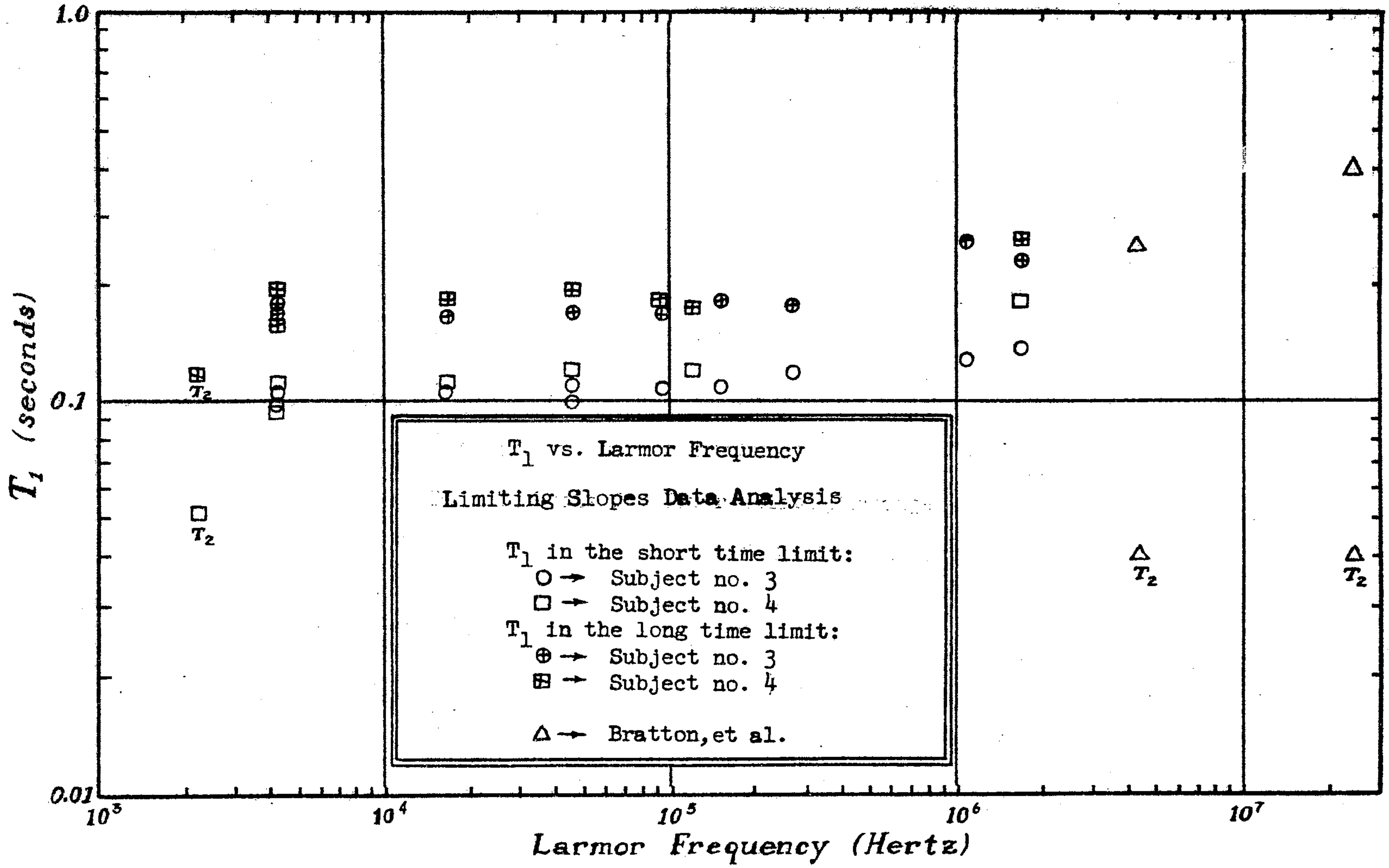

Figure 19. T_1 versus the Larmor precession frequency for limiting slopes data analysis.

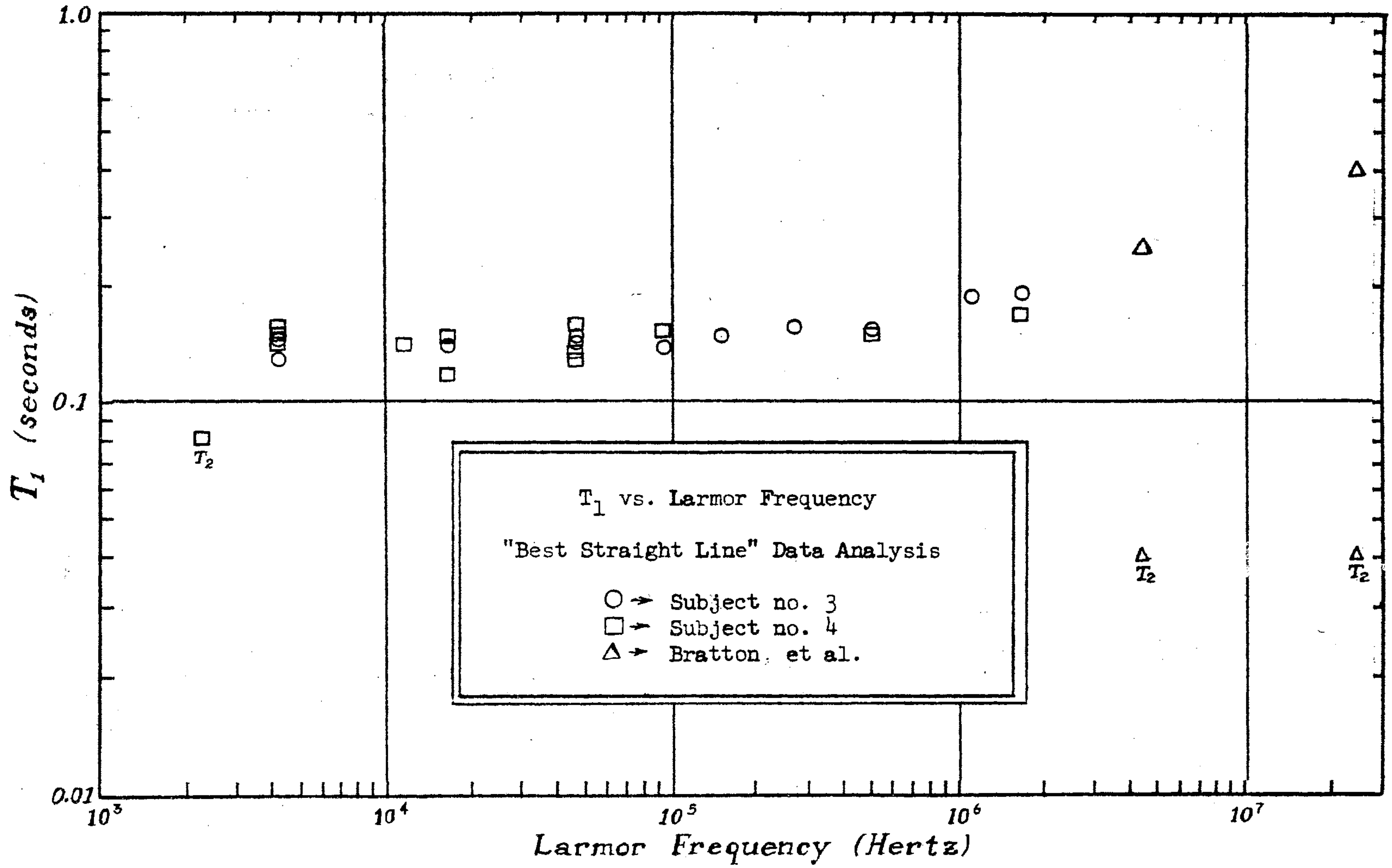

Figure 20. T_1 versus the Larmor precession frequency. Data was analyzed for the best straight line (see text).

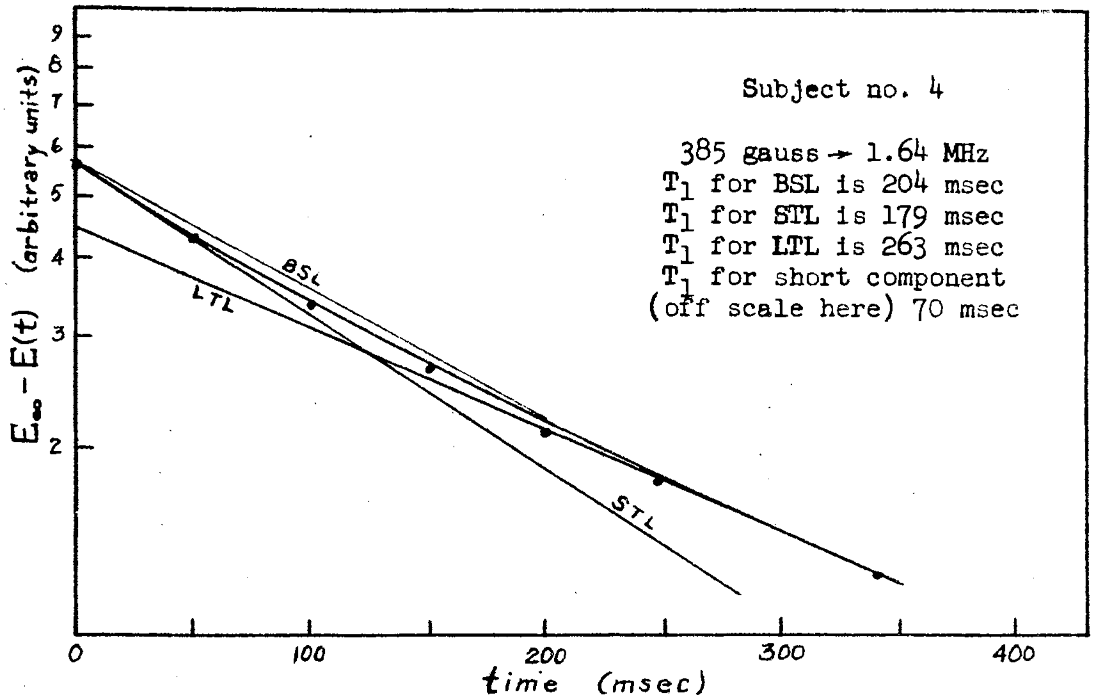

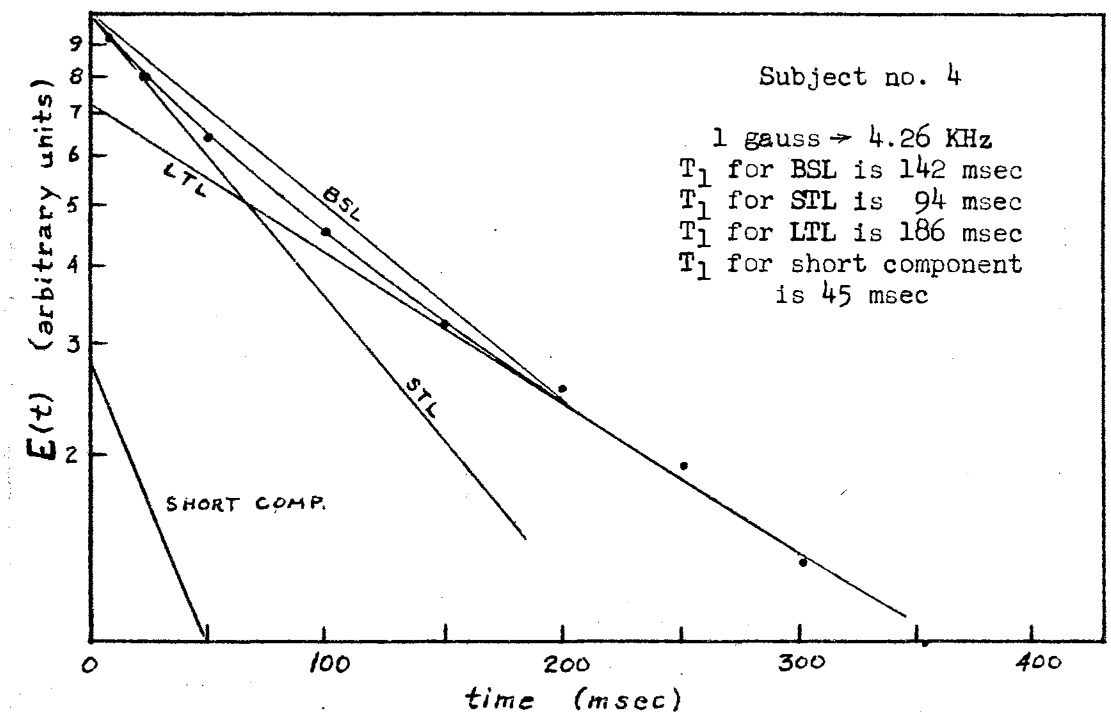

Figure 21. Typical T_1 data showing the graphical analysis.

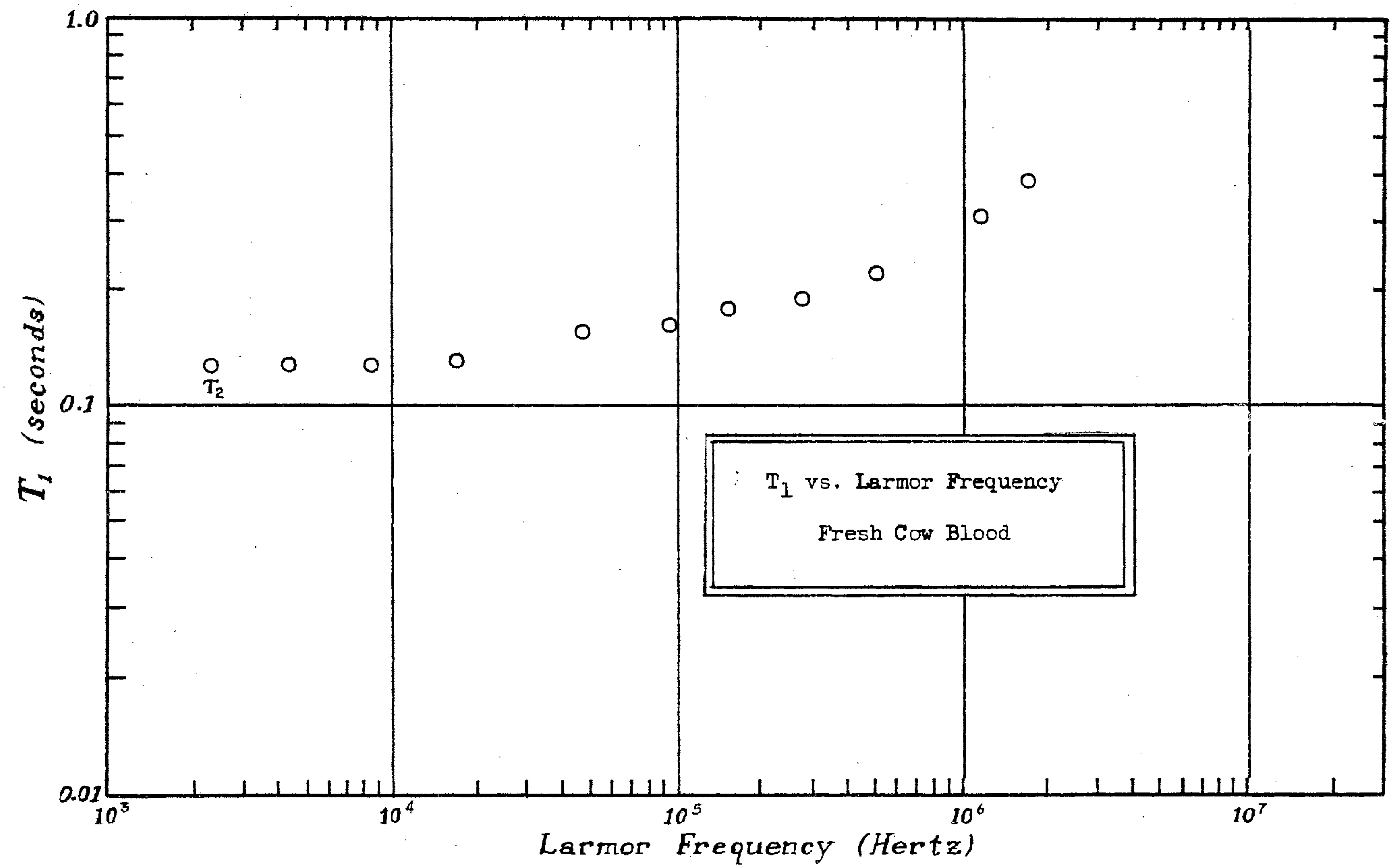

Figure 22. T_1 versus the Larmor precession frequency for cow blood.

Summary

Assuming that the nonexponential character of the T_1 and T_2 data is due to a contribution to the decay signal by protons in fat, the ideal arm for NMR studies would be one that is lean and can fit all the way into the coil,completely filling it. Though most of the water in the forearm is in muscle and the proportion of the forearm segment that is muscle is good (around 60%), due to the tapered shape of the forearm the total muscle volume is low. One shortcoming of the human arm as a muscle sample is that the degree of voluntary contraction is small and it would probably be difficult to see any effects of contraction on the relaxation times. However if exhaustion of the arm muscles by cutting off the blood supply for a short length of time would prove practical, the above would not be too much of a disadvantage. Such measurements were not attempted.

Apparently the phase model for water in muscle favored by Bratton, Hopkins and Weinberg is inadequate. Neither of the components of the T_1 decay are as low at low fields as their model predicts. If the long time component is due to water in the muscle, this water may be in two or more phases between which there is fast exchange, but T_1 reaches a plateau of about 170 msec from around 500 KHz down to at least 4.7 KHz, Larmor precession frequency. The interpretation of T_2 measurements (short component about 30 msec and a long time component of 118 msec) in the earth's field is not clear since Bratton, et al., recorded such a low value for T_2 at high fields.

General Remarks

The similarity of T_1 field dependence of blood to that of muscle is interesting. If in the muscle the water molecules associated with or in close proximity to any cell substructure constitute a phase, then the major phases present in the muscle would probably be those associated with the cell membrane and with the myofibrils, since these make up the bulk of solid matter in the muscle. Both of these structures play a major role in the process of contraction. The author feels that it would be instructive to make T_1 field dependence measurements on both whole blood and plasma. Any difference in the results must be accounted for by the presence or absence of the red blood cells. It might therefore be possible to relate a solid-like phase to those water molecules that are, for instance, in the cell walls of the erythrocytes.

In regard to the apparatus, certainly a coil of larger core diameter is needed. A core diameter of four inches would probably be big enough to admit the average arm. It would also be good to have a skin electrode that could be taped on the subject to ground him. The windings of the coil core definitely need to be sealed water tight with some abrasive-resistant compound; though all sessions were carried out in the early morning or the evening, the subjects' arms sometimes perspired. This was due as much to the fact that the polarizing coil got hot after a period of time as from the heat of the day. Though the arm was always separated from the windings by a cloth, the subject occasionally got shocked. More important from the standpoint of the experiment, this moisture apparently greatly reduced the Q of the coil, and therefore the gain of the system.

This probably accounts for the discrepancy in signal amplitudes measured on the same subject on different occasions.

A SELECTED BIBLIOGRAPHY

Bratton, Clyde B., A.L. Hopkins, and Joseph W. Weinberg. "Nuclear Magnetic Resonance Studies of Living Muscle." Science, CXLVII (February, 1965), 738-739.

Dole, Vincent P. "Body Fat." Scientific American, CCII (December, 1959), 70-76.

Dwight, Herbert Bristol. Electrical Coils and Conductors. New York: McGraw-Hill Book Company, Inc., 1945.

Ernst, E. Biophysics of the Striated Muscle. Budapest: Akademiai Kiado, 1963.

Hollinshead, W. Henry. Functional Anatomy of the Limbs and Back. Philadelphia: W.B. Saunders Company, 1960.

Huxley, H.E. "The Contraction of Muscle." Scientific American, CXCIX (November, 1958), 66-82.

__________. "The Mechanism of Muscular Contraction." Scientific American, CCXIII (December, 1965), 18-27.

Paul, W.M., E.E. Daniel, C.M. Kay, and G. Monckton, eds. Muscle. Oxford: Pergamon Press, Ltd., 1965.

Spector, William S., ed. Handbook of Biological Data. Philadelphia: W.B. Saunders Company, 1965.

Welsby, V.G. The Theory and Design of Inductance Coils. Great Britain: John Wiley and Sons, Inc., 1960.

Wolf, A.V. "Body Water." Scientific American, CXCIX (November, 1958), 125-132.

APPENDIX

DEVELOPMENT OF AN EXPRESSION FOR THE Q OF A COIL

The following circuit was used for Q measurements of the coils (see page 17):

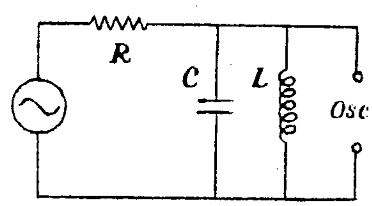

The equivalent circuit for the capacitor and inductor in parallel and with the oscilloscope across the tank was considered to be the following:

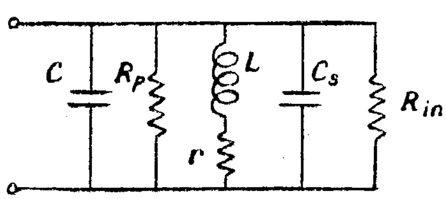

C = tuning capacitor
R_p = effective shunt resistance of tuning capacitor and
$R_p = \frac{X_c}{\delta}$ where δ = dissipation factor for the tuning capacitor
L = inductance of coil
r = lumped ac and dc resistance of coil
C_s = self-capacitance of coil
R_{in} = input resistance of a voltage measuring

Total impedance into which the signal generator feeds is

$z_{circuit} = R + z$ where

$$z = \frac{X_c X_{c_s} R_p R_{in} (X_L + r)}{X_c X_{c_s} R_p R_{in} + X_c X_{c_s} R_p (X_L + r) + X_c X_{c_s} R_{in} (X_L + r) + X_c R_p R_{in} (X_L + r) + X_{c_s} R_p R_{in} (X_L + r)} \quad \text{eq. (1)}$$

The capacitive reactance of the circuit is $\frac{1}{\omega(C+C_s)}$ and if the circuit is at resonance so that

$$X_L = X_{c+c_s}$$

then the expression for z can be put into the following form:

$$z \text{ (at resonance)} = z_r = \frac{[X_L^2 - jrX_L] R_p R_{in}}{rR_p R_{in} + (R_p + R_{in}) [X_L^2 - jrX_L]} \quad \text{eq. (2)}$$

If the coil has a high Q so that $\omega L >> r$ then the imaginary terms can be dropped and eq. (2) becomes

$$z_r = \frac{X_L^2 R_p R_{in}}{rR_p R_{in} + (R_p + R_{in}) X_L^2} \quad \text{eq. (3)}$$

$Q = \frac{X_L}{r}$ where Q is the true value for the coil. Solving eq. (3) for $\frac{X_L}{r}$ results in the expression:

$$\frac{X_L}{r} = \frac{z_r R_p R_{in}}{X_L (R_p R_{in} - zR_p - zR_{in})} = Q.$$

Making the substitution $\frac{X_c}{\delta} = R_p$:

$$Q = \frac{z_r X_c R_{in}}{X_L (X_c R_{in} - zX_c - xR_{in}\delta)}$$

which is the expression given in the text for calculating the coil Q with the relative voltages across R and z_r measured.

VITA

Thomas Richard Ligon

Candidate for the Degree of

Master of Science

Thesis: COIL DESIGN FOR LOW FIELD NMR EXPERIMENTS AND NMR MEASUREMENTS ON THE HUMAN ARM

Major Field: Physics

Biographical:

Personal Data: Born in Wewoka, Oklahoma, September 26, 1941, the son of J. David and Louise Briggs Ligon.

Education: Attended grade school in Wewoka, Oklahoma; attended high school in Norman, Oklahoma, and was graduated from Wewoka High School in 1959; attended Washington and Lee University and the University of Oklahoma, and received the Bachelor of Science degree from Oklahoma State University in May, 1964, with a major in physics. Completed the requirements for the Master of Science degree in May, 1967.

Professional Experience: Served as graduate assistant in physics at Oklahoma State University from September, 1964 to June, 1966; member of Sigma Pi Sigma honorary physics fraternity.